A STUDY ON THE PERFORMANCE OF HOLE-ENTRY HYBRID JOURNAL BEARINGS OPERATING IN TURBULENT REGIME

A DISSERTATION

submitted in partial fulfilment of the requirements for the award of the degree

of

MASTER OF TECHNOLOGY

in

MECHANICAL ENGINEERING

(with Specialization in Machine Design Engineering)

by

DEVENDRA SANKLA

DEPARTMENT OF MECHANICAL AND INDUSTRIAL ENGINEERING
INDIAN INSTITUTE OF TECHNOLOGY ROORKEE
ROORKEE - 247 667 (INDIA)

JUNE, 2011

INDIAN INSTITUTE OF TECHNOLOGY

ROORKEE

CANDIDATE'S DECLARATION

I hereby declare that the work which is presented in this dissertation entitled "**A STUDY ON THE PERFORMANCE OF HOLE-ENTRY HYBRID JOURNAL BEARINGS OPERATING IN TURBULENT REGIME**", submitted in partial fulfillment of the requirements for the award of the degree of **MASTER OF TECHNOLOGY** in **Mechanical Engineering** with specialization in **MACHINE DESIGN ENGINEERING** is an authentic record of work done by my own efforts with suitable acknowledgement to all references. This work has been carried out by me at **Department of Mechanical and Industrial Engineering, IIT Roorkee,** from July 2010 to June 2011, under the supervision of **Dr. Satish C. Sharma, Professor** and **Head,** Department of Mechanical and Industrial Engineering, IIT Roorkee.

I have not submitted the matter embodied in this report for the award of any other degree or diploma to any other institute or university.

Date: 29/06/2011

Place: Roorkee

DEVENDRA SANKLA

CERTIFICATE

This is to certify that the above statement made by the candidate is true, to the best of my knowledge and belief.

29/06/11

Dr. Satish C. Sharma

Professor & Head,

MIED, IIT Roorkee.

ACKNOWLEDGEMENT

I would like to express my sincere thanks, immense pleasure and gratitude to **Dr. Satish C. Sharma**, **Professor** and **Head,** in Department of **Mechanical and Industrial Engineering, IIT Roorkee** for his whole-hearted support and guidance. This work is simply the reflection of his thoughts, ideas and concepts. I am deeply indebted to him for his valuable insights and directions that encouraged me to complete the project successfully in allotted time. Working under his guidance was a privilege and an excellent learning experience that I will cherish throughout my life.

I am especially grateful to Mr. Nathi Ram, Research Scholar, MIED, IIT Roorkee for their valuable guidance and affection that boost up my skills to bringing out this dissertation report.

I would like to express our thanks and gratitude to my colleague Mr. Arvind Kumar Rajput for motivation and support to complete present work.

I would like to express our thanks and gratitude to the staff of Tribology Lab, Mr. Loti Ram, for his support and motivation in completion of my work.

I am very thankful to my parents & all of my friends for their never ending encouragement in bringing out this dissertation report to the form as it are now.

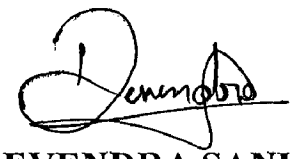

Date : 29/06/2011

Place: Roorkee

DEVENDRA SANKLA

(M/C DESIGN ENGINEERING)

ENROL. No. - 09539005

ABSTRACT

Bearings are used extensively in all rotating machinery in the industry to support load. Their performance plays an important role in chemical, petrochemical, automotive, power generation, aerospace, turbo machinery and process industries. Bearings are generally designed based on empirical relations and design charts. The pioneering work in this field has been done by W. B. Rowe and co-workers. In present time the machines are required to be operated under very stringent, exact and precise conditions so as to cope with the latest technology advancement and constraints. Therefore the bearings are designed on the basis of more accurately predicted design data.

Non-recessed hole-entry hybrid journal bearing system, which gives improved performance over recessed hybrid journal bearings, are successfully used in many engineering applications. The non-recessed bearing system especially the hole-entry hybrid journal bearings provide excellent performance such as low power consumption, increased minimum fluid film thickness, large fluid film damping and relatively simplicity in manufacturing. These features make these bearings more suitable for many engineering applications such as reactor coolant pump, liquid rocket engine etc.

The phenomenon of turbulence in lubrication has been received increasing attention from many researchers. Turbulence occurs basically for two reasons; high speed operation, and the use of unconventional lubricants of low kinematic viscosity such as water, synthetic lubricants or liquid metals. Sometimes the process fluids of low kinematic viscosity are used as lubricants to simplify the equipment design or to overcome the difficulty of shaft sealing. A high velocity combined with low kinematic viscosity leads to high Reynolds number generates a turbulent flow.

The performance of non-recessed hole-entry hybrid journal bearing systems gets affected by number of parameters such as types of restrictor, mode of operation of bearing and wear. The wear occurs due to frequent (start/stop) operations in journal bearings. During the transient periods, the bush progressively wears. The wear could be large and may significantly alter the bearing performance depending upon bearing material and applied load. Therefore, the influence of wear on the performance of bearing characteristics is quite significantly. The present work is

aimed to study theoretically, the influence of turbulence and wear on the performance characteristics of a non-recessed hole-entry hybrid journal bearing system.

For computing the bearing performance characteristics, the wear caused on the bearing surfaces is modeled using Dufranes's abrasive wear model. The modified Reynolds equation based on Constantinescu's lubrication theory has been solved using FEM together with restrictors flow equations as a constraint. The numerically computed results have been presented for bearing operating and geometric parameters, for various values of Reynolds number and conclusions has been drawn for non-recessed hole-entry hybrid journal bearing system.

CONTENTS

NOMENCLATURE

DIMENSIONAL PARAMETERS

C_f Coefficient of friction

C_{ij} Fluid film damping coefficient

D Diameter of journal, mm

F Fluid film reaction $\{\frac{\partial h}{\partial t} \neq 0\}$, N

F_o Fluid film reaction $\{\frac{\partial h}{\partial t} = 0\}$, N

L Bearing height, mm

Q Bearing flow, mm^3s^{-1}

R_j Radius of journal, mm

R_b Radius of bearing, mm

R_e Reynolds number

R_e^* Local Reynolds number $\left(\frac{\rho h}{\nu}\right)$

M Mass parameter

W_o External load, N

S_{ij} Fluid film stiffness coefficient

X, Y, Z Cartesian coordinates

X_j, Z_j Coordinates of steady-state equilibrium journal centre from geometric centre of bearing, mm

a Radius of capillary, mm

a_b Bearing land width, mm

c Radial clearance, mm

e Journal eccentricity, mm

h	Fluid film thickness, mm
l	Characteristic length, mm
l_c	Length of capillary, mm
p	Pressure, Nmm^{-2}
p_c	Pressure at hole, Nmm^{-2}
p_s	Supply pressure, Nmm^{-2}
τ	Time, s

GREEK SYMBOLS

λ	Aspect ratio, L/D
μ	Dynamic viscosity of lubricant, Nsm^{-2}
μ_r	Dynamic viscosity of lubricant at reference temperature & pressure, Nsm^{-2}
ρ	Density of lubricant, $kgmm^{-3}$
ω_j	Journal rotational speed, rad. s^{-1}
δ_w	Wear depth, mm
ω_{th}	Threshold speed, rad. s^{-1}
ψ_d	Coefficient of discharge for orifice

NON-DIMENSIONAL PARAMETERS

$\bar{C}_{ij}$	$C_{ij}(c^3/\mu R_j^4)$
$\bar{C}_{s2}$	Restrictor design parameter
$\bar{F}$	$(F/p_s R_j^2)$
$\bar{F}_o$	$(F_o/p_s R_j^2)$
$\bar{M}$	Non-dimensional mass parameter, $\bar{M}=M_c\omega_j^2/W_o$
$\bar{M}_c$	Critical value of mass parameter
$\bar{M}_j$	Non-dimensional journal mass parameter

$\bar{Q}$	$Q(\mu/c^3 p_s)$
$\bar{S}_{ij}$	$S_{ij}\left(\frac{c}{p_s R_j^2}\right)$
$\bar{W}_o$	$W_o / p_s R_j^2$
$\bar{X}_j$	X_j/c
$\bar{Z}_j$	Z_j/c
$\bar{a}_b$	Land width ratio, a_b/L
$\bar{h}$	h/c
$\bar{h}_{min}$	h_{min}/c
$\bar{p}$	p/p_s
$\bar{\tau}$	$\tau\ (c^2 p_s/\mu R^2_j)$
Ω	Speed parameter, $\omega_j\ (\mu R^2_j/\ c^2 p_s)$
α	Circumferential coordinates, (X/R_j)
β	Axial coordinates, (Y/R_j)
$\varepsilon, \varepsilon_o$	Eccentricity ratio, e/c
$\bar{\mu}$	μ/μ_r
$\bar{\omega}_{th}$	ω_{th}/ω_I
$\bar{\delta}_w$	Wear depth parameter, δ_w/c

MATRICES AND VECTORS

N_i, N_j	Shape functions
$[\bar{F}]$	Fluidity matrix
$[J]$	Jacobian matrix
$\{\bar{Q}\}$	Nodal flow vector
$\{\bar{R}_H\}$	Vector due to hydrodynamic term

$\{\bar{R}_{xj}\}$, $\{\bar{R}_{zj}\}$ Vector due to journal centre velocities

$\{\bar{p}\}$ Nodal pressure vector

SUBSCRIPTS AND SUPERSCRIPTS

J Journal

R Restrictor

c Pocket

o Steady-state solution

s Supply pressure

— Corresponding non-dimensional parameter

***** Concentric operator

LIST OF FIGURES

LIST OF TABLES

CHAPTER- 1 INTRODUCTION

The name tribology was coined in 1967 by D. Dowson. The word "tribology" came from the Greek word "tribo" means to rub and "logos" means principal or logic. In another way it is also defined as "Tribology is the science which deals with the relative motion between interacting surfaces" or "Tribology is a basic applied discipline that primarily studies friction, wear, and lubrication". Friction is a principal cause of wear and energy dissipation. It is estimated that one third of world's energy resources in present use in needed to overcome friction that one form or another. Lubrication is an effective means of controlling wear and reducing friction. According to an estimate in India alone Rs 6000 cores are wasted annually due to improper tribological practices. The tribological science is playing an important role in the improving the quality of people's life, there by having an important impact on the sustainable development of the national economy. It is a very practical subject where saving resources and energy and improving economic efficiency are its main goal. The study of tribology is commonly applied in bearing design but extends into almost all other aspects of modern technology, such as metal working processes, rolling mills, medical equipments and turbines in power plants. An advanced application of tribology found in lubrication of hip implants and other artificial prosthesis.

Turbulent flow may occur in bearings due to two main reasons. The first is high-speed operation required in modern machinery. The second is the use of unconventional lubricants such as water or liquid metals due to the need to simplify equipment design or to overcome the difficulty in shaft sealing. A high velocity with a low kinematic viscosity leads to higher Reynolds numbers and as a result departure from laminar flow conditions takes place. Some applications of turbulent lubrication are oil lubricated bearings in large power plants, water lubricated bearings and a cryogenic bearings. It may be observed that, at higher Reynolds number there is a significant increase in the friction and change in pressure and temperature

Scholars and specialists in tribological research have proven that wear is one of main reasons for damage to materials according to statistics from England, the United States and Germany, the economic loss related to friction and wear costs about 2-7 percent of GDP. A

report by the U.S. Department of Energy in 1999 pointed out that by adopting measures to reduce friction and wear, America's motor vehicle and transmission system saves 120 billion US dollars each year. In UK alone, the losses in the year 2001 due to one percent of these losses can potentially be saved by the application of know techniques to reduce friction and wear in machines. The cost benefit ration for research to generate improvement is believed to be about 1:50. The statistics reveals the usefulness of wear related studies. Although the focus of wear related studies are aimed towards improvement of quality of materials, still the wear caused due to transient (start/stop) is inevitable. The wear caused by these operations may influence bearing performance and in turn may affect the bearing life.

Since in the present times, the machines are required to be operated under very stringent, exact and precise conditions so as to cope with the latest technology advancements and constraints, therefore, the bearings are designed on the basis of more accurately predicted design data. So in order the estimate the performance of the bearings, lubricant must be taken into account.

1.1 FUNDAMENTALS OF JOURNAL BEARINGS

Fluid film bearings are classified by the principle of operation, the direction of loading and type as follows.

Classification by Operation Principle

- Hydrodynamic bearings produce oil film pressure to support a load by rotation inside the bearing.
- Hydrostatic bearings support a load by the pressure is supplied by an outside source.
- Hybrid bearings are the bearings support the load by combined hydrodynamic and hydrostatic action.

Classification on The Basis of Direction of loading

- If journal bearings support a load acting in the direction normal to the rotating shaft. It is called journal bearings because the neck of the shaft is called a journal. It is the most common bearing among sliding bearings.
- Thrust bearings support a thrust, or load acting along the axis of the shaft.
- Yates bearings which take both thrust and radial loads.

1.1.1 HYDROSTATIC/ HYBRID JOURNAL BEARINGS

The development of externally pressurized bearings has progressed over approximately 150 years since L.D. Girard invented hydrostatic bearing in 1851. From that date externally pressurized journal bearings have increased in use in engineering application such as;

- Test equipment
- Medical equipment
- Machine tools
- High speed turbo machinery
- Measuring instruments and in aerospace industry.

Their popularity is attributed to their high load-carrying capacity, zero starting friction and low friction at low speeds, nominally less wear and hence long life, good rotational accuracy and excellent stiffness and damping.

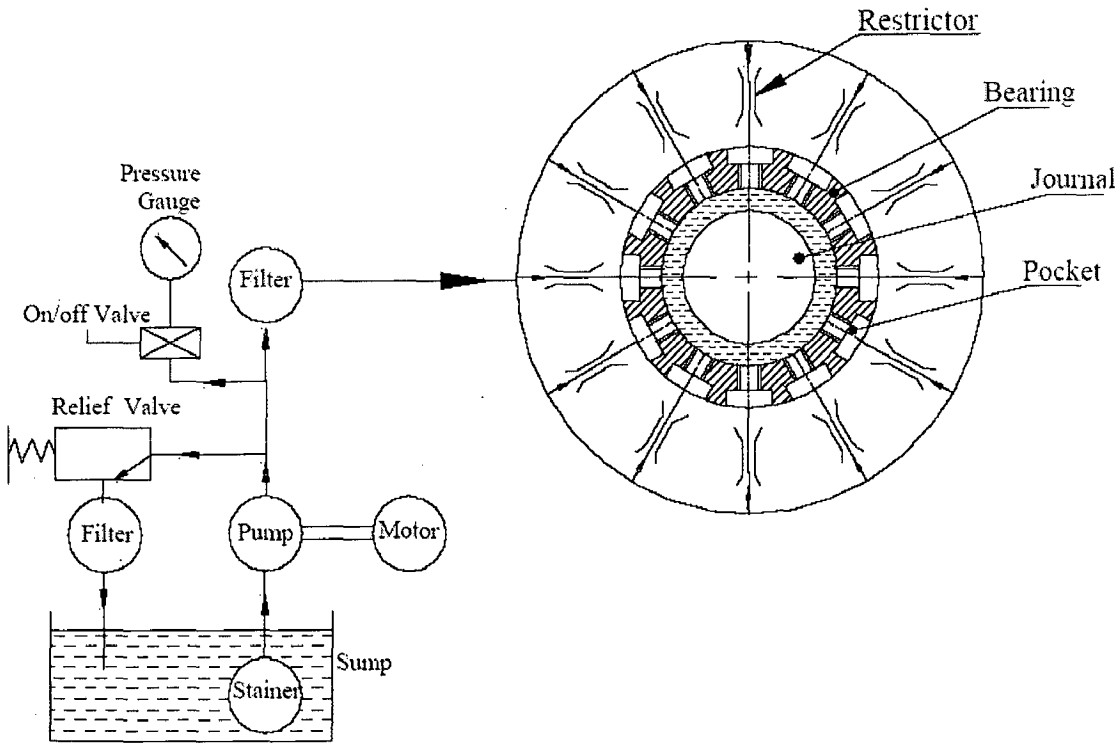

Fig 1.1 Operation of multiple hole-entry hybrid journal bearing

The principle operation of these bearings is that the bearings surfaces are separated by a film of lubricant supplied under pressure to the bearing via restrictors or compensating elements

i.e. capillaries, orifices and constant flow valves etc. The basic operating principle of a hydrostatic /hybrid journal bearings system is shown in Fig 1.1. A capillary restrictor is generally very long in relation to its cross sectional dimensions where as an orifice restrictor is very short. The resistance to flow of fluid through a capillary restrictor depends essentially on the shear stress developed the fluid as a consequence of its viscosity; whereas the resistance to flow of fluid through an orifice restrictor is developed as a consequence of fluid inertia or density.

A hybrid journal bearing basically combines the mechanism of hydrostatic and hydrodynamic principles in a bearing to achieve load support at low as well as high speeds and provide superior performance as compared to hydrostatic journal bearing. Basically the hybrid journal bearing configurations are classified into two group's namely recessed (pockets) and non-recessed (plain) journal bearings.

Non-recessed hybrid journal bearings configuration is of two types. The first one is the hole-entry in which two rows of six or more holes are provided around the circumference of the bearing either symmetrically or asymmetrically as shown in Fig 1.2 (a) and Fig 1.2 (b) respectively the other type of non-recessed hybrid journal bearing is known as slot-entry bearing as shown in Fig 1.3 (a) and Fig 1.3 (b) use of this kind of bearing is used in application such as grinding wheel spindle.

The design of hydrostatic/hybrid bearings is a complex process and it includes number of parameters. However, the accuracy of design depends on the accurate computation of performance characteristics.

Some of the primary objectives of hybrid journal bearing designs include the following:

- To maximum load carrying capacity,
- To maximum bearing stiffness,
- To minimize bearing power dissipation,
- To minimize oil temperature rise in bearing,
- To minimize the power and size requirement of the associated hydraulic power supply.

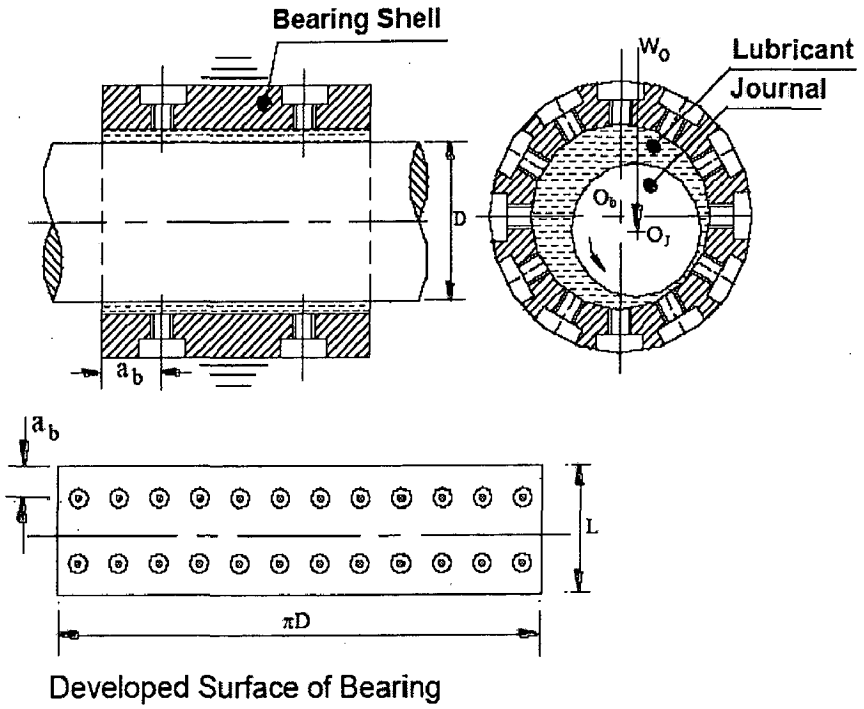

(a)

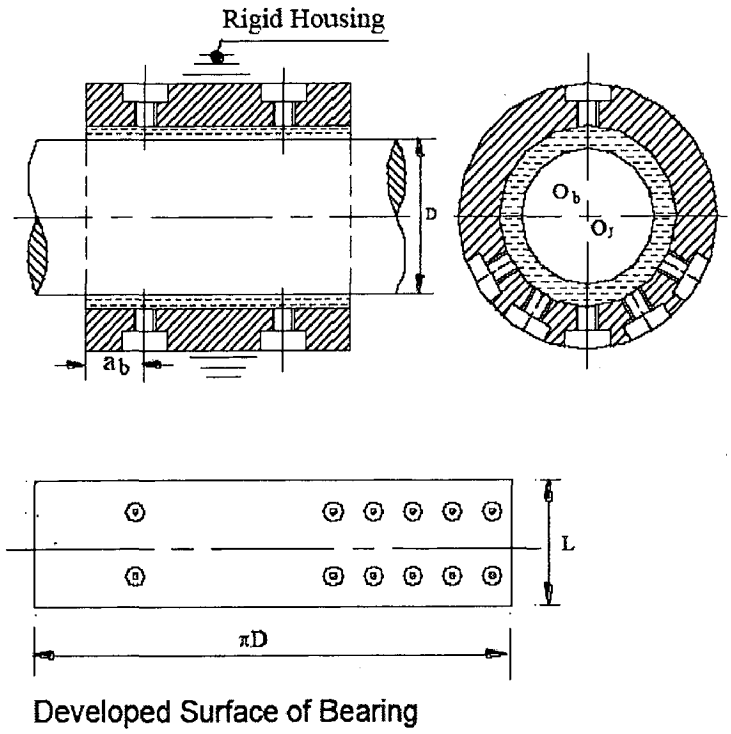

(b)

Fig 1.2: Non-recessed hole entry journal bearing (a) Symmetric bearing configuration (b) Asymmetric bearing configuration.

1.1.2 NON-RECESSED JOURNAL BEARINGS

The non-recessed journal bearings, which are commonly used in industries, are of different configurations. The two frequently used configurations normally used are hole-entry type and slot entry type. The holes, in a hole-entry bearing configuration are disposed around the circumference of the bearing in an asymmetrical or symmetrical manner having capillary or orifice compensating elements. The Fig.1.2 shows diagrammatically the geometric configuration of an externally pressurized hole-entry hybrid journal bearing. The another configuration of non-recessed journal bearing configuration which is widely used is a slot entry hybrid journal bearing configuration, and is shown diagrammatically in Fig.1.3 It is simple configuration of an externally pressurized bearing, the fluid is being fed to the bearing gap through number of narrow inlet slots, which have the same order of width as the film thickness, metering the fluid to the bearing and thereby eliminating the need of orifice restrictors.

Generally hydrostatic journal bearing configuration consists of a number of pockets or recessed in circumferential direction. But this pocket or recessed occupy a large portion of bearing area, thus generating a less hydrodynamic action under hybrid mode. Therefore to utilize both hydrostatic and hydrodynamic action in a more efficient manner and to have ease in manufacturing, the non-recessed bearing configurations were developed.

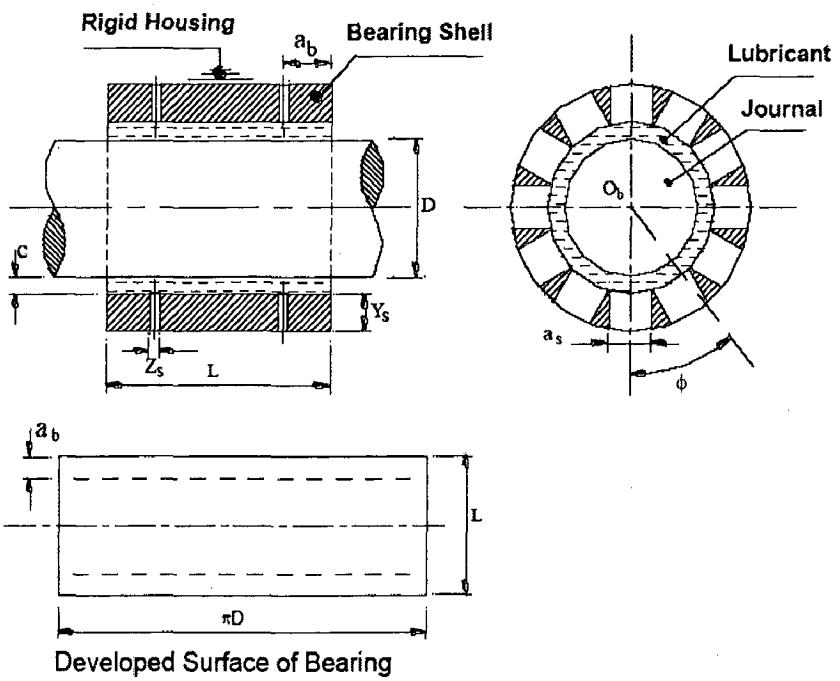

(a)

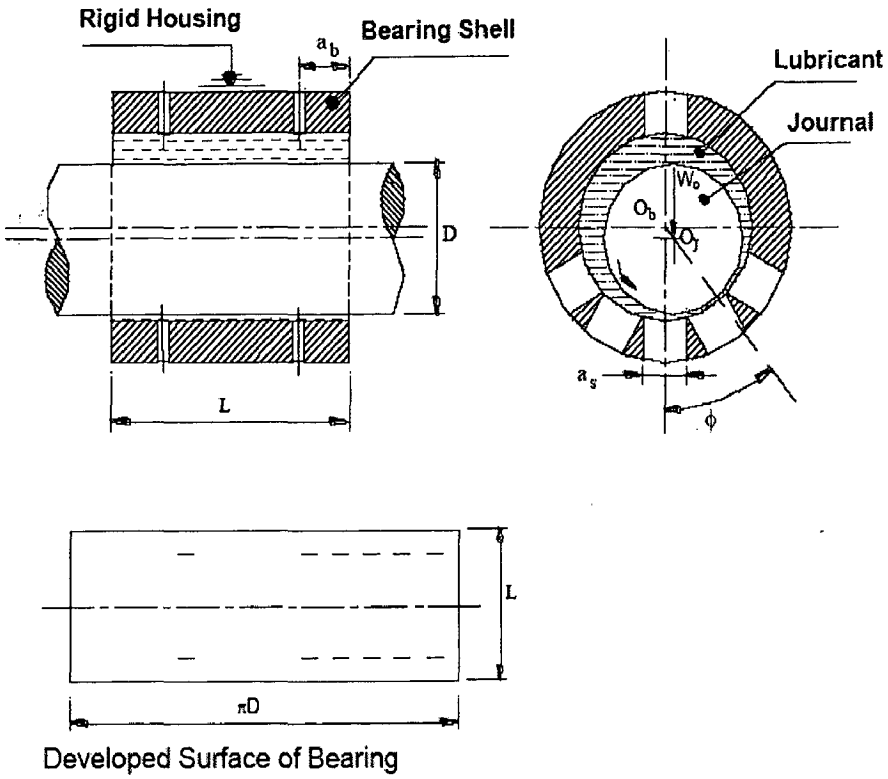

(b)

Fig 1.3: Non-recessed Slot entry journal bearing (a) Symmetric bearing configuration (b) Asymmetric bearing configuration

CHAPTER- 2 LITERATURE REVIEW

2.1 TURBULENCE IN JOURNAL BEARINGS

The phenomenon of turbulent lubrication has received increasing attention of many researchers. A turbulent flow could be defined as an irregular flow in which such quantities as fluid velocity and pressure varies randomly with respected to both space and time. In analyzing the Navier- Stokes equation for turbulent flow conditions each parameter is often represented by a time mean value with a fluctuation about this mean value. At the high values of Reynolds number a laminar mode of flow can degenerate into a turbulent one.

Turbulence occurs in bearings basically for two reasons:

1. High speed operation.
2. The use of unconventional lubricants of low kinematic viscosity such as water, synthetic lubricants or liquid metals.

Sometimes process fluids of low viscosity are used as lubricants to simplify the equipment design or to overcome the difficulty of shaft sealing. A high velocity combined with low kinematic viscosity leads to high Reynolds number, resulting in either a super laminar flow or turbulence.

2.2 TURBULENT LUBRICATION THEORIES

There are different theories proposed by the various researchers prominent among them have been described as below.

1. Constantinescu's theory

The construction of a turbulent lubrication theory has been attempted by a number of investigators for the past decades. Constantinescu originally developed a theoretical approach to such a problem based on the mixing length concept. The basic problem lies in the representation of the turbulent stresses in terms of mean velocity gradient in order to reduce the equation to a soluble form. Considering the x-coordinate direction the turbulent stress is represented by [29]

$$-\bar{\rho}\,\overline{u'v'} = \rho l^2 \frac{\partial \bar{u}}{\partial y}\left|\frac{\partial \bar{u}}{\partial y}\right| \qquad (2.1)$$

The mixing length l is related to the independent variable by means of the mixing length constant, k.

Constantinescu proposed the form of Reynolds equation in turbulent regime is represented as[29],

$$\frac{\partial}{\partial\alpha}\left[\frac{h^3}{G_\alpha\mu}\frac{\partial p}{\partial\alpha}\right]+\frac{\partial}{\partial\beta}\left[\frac{h^3}{G_\beta\mu}\frac{\partial p}{\partial\beta}\right]=\frac{U}{2}\frac{\partial h}{\partial\alpha}+\frac{\partial h}{\partial\tau} \tag{2.2}$$

where, $\frac{1}{G_\alpha}=k_\alpha$ and $\frac{1}{G_\beta}=k_\beta$ are turbulent coefficients.

Constantinescu considered strong Couette flows and hence application of his results to hybrid and hydrostatic bearings may lead to errors. By means of a linearization he indicated the following values of turbulent coefficients k_α and k_β.

$$\left.\begin{aligned} k_\alpha &= \frac{1}{G_\alpha} = 12 + 0.53(k^2\mathrm{Re})^{0.725} \\ k_\beta &= \frac{1}{G_\beta} = 12 + 0.296(k^2\mathrm{Re})^{0.55} \end{aligned}\right\} \tag{2.3}$$

Constantinescu recommends the following value for mixing length constant, k;

$k = 0.125\ \mathrm{Re}^{0.07}$

Then the values of k_α & k_β becomes,

$$\left.\begin{aligned} k_\alpha &= \frac{1}{G_\alpha} = 12 + 0.0260\mathrm{Re}^{0.8265} \\ k_\beta &= \frac{1}{G_\beta} = 12 + 0.0198\mathrm{Re}^{0.741} \end{aligned}\right\} \tag{2.4}$$

For laminar flow the value of k_α and k_β is 12.

2. Ng, Pan and Elrod's theory

Ng and Pan utilized the concept of eddy viscosity to represent the turbulent stresses in term of mean velocity gradient. Thus in x-direction the turbulent stress becomes,

$$-\bar{\rho}\,\overline{u'v'}=\rho\,\varepsilon\frac{\partial\bar{u}}{\partial y} \tag{2.5}$$

Where, ε is known as eddy diffusivity.

Initially the work of Ng and Pan was also concerned with strong Couette flows and values of k_α & k_β were presented in following expressions as [29],

$$\left.\begin{aligned} k_\alpha &= \frac{1}{G_\alpha} = 12 + k_1\,\mathrm{Re}^{n_\alpha} \\ k_\beta &= \frac{1}{G_\beta} = 12 + k_2\mathrm{Re}^{n_\beta} \end{aligned}\right\} \qquad (2.6)$$

The work of Ng and pan was extended by Elrod and Ng with application to turbulent hydrostatic and hybrid bearings.

3. Hirs theory

After the Constantinescu and Ng, Pan and Elrod a new theory developed by Hirs. This theory based on bulk flow approach which requires no physical representation of the turbulent transport mechanism. A particular advantage of the approach is that empirical constants used in the theory can be derived from the bulk flow measurement without the determination of velocity profiles. Consequently there is no recourse to the scheme adopted by others to represent the turbulent stresses in terms of the mean velocity gradient.

An empirical relation developed by Hirs given as [29],

$$\frac{\tau^*}{\frac{\rho u m^2}{2}} = n\left(\frac{\rho h u_m}{\mu}\right)^m \qquad (2.7)$$

where, u_m= mean flow velocity relative to the well where the shear stress τ^* is exerted. The constants n and m are determined from experimental results.

For the strong Couette flow Hirs gives the following values for k_α and k_β for smooth surface and Reynolds number less than 10^5,

$$\left.\begin{aligned} k_\alpha &= \frac{1}{G_\alpha} = 0.0687\,\mathrm{Re}^{0.75} \\ k_\beta &= \frac{1}{G_\beta} = 0.0392\,\mathrm{Re}^{0.75} \end{aligned}\right\} \qquad (2.8)$$

The values of k_x and k_z must not be fall below 12. The limiting Reynolds number for this situation is given as [29],

k_α = 12 when Re = 977

k_β = 12 when Re = 2060

These theories are convenient to use and they yield substantially similar results.

Some conclusion comes out from the study of previously mentioned theories.

- The above mentioned three theories yield the same form of Reynolds equation. But they get different values of turbulent coefficients k_α and k_β.
- It has been noted that the Constantinescu's theory takes less computational time.
- Constantinescu's theory easy to understand and simple in application.
- Constantinescu's theory can also be applied for compressible fluids.
- Constantinescu did not mention about transition zone where as later work of Ng-Pan and Elrod mentioned about transition zone.

2.3 REVIEW OF AVAILABLE LITERATURES

The review work presented in the thesis concern with the investigation on the performance of non-recessed hole-entry hybrid journal bearing operating in turbulent regime. Over the last few decades numerous studies on the hydrostatic/hybrid fluid film journal bearings have been carried out and reported in the literature. Since the available literature in the area of fluid film journal bearings is quite vast and abundance and rather difficult to present all these information. Therefore, in this chapter only the relevant literature, which concerns with the present study have been reviewed. The available studies in this chapter have been arranged in subsequent paragraphs.

2.3.1 THE STUDIES RELATED TO HYDROSTATIC/HYBRID JOURNAL BEARINGS

In recent times the non-recessed journal bearing configurations have been investigated thoroughly. In following section, some of important studies concerning these classes of bearings have been reviewed and discussed:

A theoretical analysis of hole-entry hybrid journal bearing system employing capillary restrictor has been presented by Yoshimoto [1]. The finite difference method was used to solve to Reynolds's equation, replacing the negative pressure by P = 0 for the cavitated region. Results were presented for bearings with various pocket size. From the results if was found that the load capacity of this type of bearing is greatly affected by the pocket size at zero and high speeds.

Rowe et al. [2] studied the performance characteristics of hybrid journal bearings with particular reference to hole-entry configurations. A modification to the procedure for solving the Reynolds equation is introduced to cope with cavitated regions. The performance characteristics of slot-entry were compared with hole-entry and recessed bearings for different power ratios. They concluded that hole-entry bearings offer advantages for hybrid performance and also easy to manufacture. Stout & Rowe [3] discussed the design of liquid journal bearings and compared the recessed and non-recessed bearings, showing that slot-entry bearings offer greatest load capacity up to 0.5 eccentricity ratio. The effects of temperature variations and manufacturing variations on bearing performance were also discussed. Rowe and Koshal [4] presented a design strategy for hybrid journal bearings which deals with maximum load for minimum total power dissipation. A new technique for optimizing hybrid journal bearings was presented. Their method involved the comparison of bearings to be optimized with a reference bearing on the basis of load/total power, load/pumping power and load/flow. They concluded that substantial increases in load support can be achieved with significant reduction in total power dissipation through the design for hybrid operation. Cheng and Rowe [5] presented a selection strategy for the design of externally pressurized journal bearings. The strategy concerned the selection of bearing type and configuration, the fluid feeding device and bearing material. A selection model was proposed, which can be applied to the selection of bearing type, configuration and fluid feeding device. They concluded that the approach can be extended to develop a general computerized system for design of bearings of a wide variety of types. Stout and Rowe [6] aimed to achieve the five basic goals in their study related to the selection of bearing configurations, geometry, control devices and materials, for both gas and liquid fed bearings. The goals were correct tolerance, minimum tool power dissipation, low temperature, total system design and material selection. They concluded that recessed bearings are best suited for minimizing power dissipation and temperature rise, while non-recessed bearings are best suited for high-speed applications since they perform well as hybrid bearings. Sharma et al. [7] presented the performance characteristics of externally pressured hole-entry hybrid journal bearings with capillary restrictor analytically. The finite element method had been used to solve Reynolds equation. The bearing performance characteristics are presented for a wide range of values of deformation coefficient. The performance characteristics were compared for two hole-entry bearing configurations. They concluded that value of maximum pressure, minimum film thickness altitude angle and damping

coefficients decreases with an increase in bearing flexibility for both the configurations studied. Sharma et al. [8] described the performance of slot entry hydrostatic/hybrid journal bearing by considering bearings shell flexibility the analysis. The relevant governing equations were solved by finite element method. Slot entry journal bearings of two separate configurations were studied over a wide range of bearing's operating and geometric parameters. Elastic effects were found to significantly affect the bearing. Sharma et al. [9] presented a theoretical study concerning the static and dynamic performance of hydrostatic/hybrid journal bearings compensated by slot restrictor. The results were presented for double row symmetric as well as asymmetric configurations for different values of slot width ratio and external load. Sharma et al. [10] presented a theoretical study concerning the journal misalignment effect on the static and dynamic performance characteristics of a capillary compensated hole-entry hybrid journal bearing. The static and dynamic performance characteristics are presented for the different representative values of journal misalignment parameters for both hydrostatic and hybrid mode of operations. It has been demonstrated that the reduction in minimum fluid-film thickness due to journal misalignment can be partially compensated by the appropriate selection of restrictor design parameter. The study indicates that the journal misalignment significantly affects the performance of the hole-entry journal bearing and for a more accurate prediction of the bearing performance it is suggested to be considered in the analysis for an accurate prediction of the bearing performance. Sharma et al. [11] studied theoretically the performance of a hole-entry hybrid journal bearing system by considering variation of viscosity due to temperature rise of the lubricant. The results presented by them indicates that the variation of viscosity due to temperature rise of the lubricant fluid-film have a quite appreciable influence on the static and dynamic performance of a hole entry hybrid journal bearing system. Vijay et al. [12] investigated the influence of viscosity variation due to temperature on the stability parameters of constant flow valve compensated hole-entry bearing and found out that the bearing performance characteristics are greatly affected and thus a designer should select an optimum value of bearing design parameters. Awasthi et al. [13] studied the performance characteristics for an orifice compensated hole-entry hybrid journal bearing having configuration of uniform distribution of holes in the circumferential direction. The results show that the wear affects the bearing performance significantly. Therefore, consideration of wear defect should be given for an accurate prediction of the bearing performance over a number of cycles. Awasthi et al. [14]

carried out study on the performance of worn non-recessed hole-entry hybrid journal bearing system. The results of bearing performance characteristics parameters in terms of maximum fluid-film pressure, minimum fluid-film thickness, flow rate and stability threshold speed, etc have been presented. The results indicate that the wear affect the bearing performance considerably. Ives and Rowe [15] carried their work on theoretical investigation of slot-entry hybrid journal bearing operating in super laminar flow regime. Their work consist the effect of super laminar flow on the optimization of slot-entry hybrid journal bearing system. They concluded that the main effect of operating in the super laminar flow regions on bearings performance was to greatly prediction of friction power. Constantinescu [16] analyzed theoretically three dimensional motions in the lubricant layer by using Prandtl's mixing length theory. He presented calculations for journal and thrust bearings subjected to turbulent lubrication. Constantinescu [17] studied the transient conditions from laminar to turbulent regime for gas lubricated bearings. He developed a method to determine the pressure and the operating characteristics for a high bearing number. From the results, he showed that turbulence does not alter quantitatively the operating conditions of gas lubricated bearings. Constantinescu and Galetuse [18] developed mixing length theory for determining the velocity profile and pressure distribution in turbulent fluid film, later same theory used for determining the friction stresses. They also used same formula for calculation of the friction forces and friction torques in journal bearings and slider bearings. Constantinescu [19] analyzed and come on the conclusion that thermal effects are in general less important in turbulent flow as compared to laminar and he found that all the methods studied by him, can be extended in order to evaluate the operating characteristics of fluid film bearing in transition region between laminar and fully developed turbulent flow. Constantinescu and Galetuse [20] assumed the shape of the velocity profiles is not strongly affected by inertia forces and evaluated the momentum equations for laminar and turbulent flow in fluid film bearings. Galetuse [21] performed experiments concern the turbulent motion of an air film between a rotating cylindrical surface and a fixed plane surface. From the experiments he determined the pressure distribution for the main flow direction and the lateral direction. He gave the important information regarding effect of inertia forces when the lubricant film thickness shows large variation. Constantinescu and Galetuse [22] presented data for operating characteristics of journal bearings operating in turbulent inertial flow. They found that, at least for the range of variation of the Reynolds number and the clearance ratio which might

of Routh-Hurwitz criterion by using the perturbation technique. Vohr and Mein-kai Ho [33] presented a turbulent energy model for determination of turbulent stresses is used to calculate velocity profiles in lubricant films. They showed that the results are matched with prediction of the previously established turbulent lubrication theory given by Elrod, Ng and Pan. Vohr et al. [34] discussed an analytical and experimental investigation of turbulent flow in bearing films including the effects of convective fluid inertia forces. They analyzed turbulence is treated by means of turbulent viscosity correction factor. They studied the pad bearings of arbitrary surface geometry by using a computer program to calculate the film pressure developed in such bearings. They found that good match between results. Hashimoto and Wada [35] studied turbulent lubrication of tilting-pad thrust bearings with the effect of thermal and elastic deformations. They introduced the effect of pad deformations when analyzing performances of such bearings running in the turbulent condition. Hashimoto et al. [36] worked on application of short bearing and presented theory to dynamic characteristics problem related to turbulent journal bearings. They found that the turbulence has significant effect on the dynamic behavior of rotor bearing system and the short bearing theory has an advantage of less computational time required for the calculation for the journal centre trajectories with an acceptable accuracy. Hashimoto and Wada [37] presented theoretical approach to turbulent lubrication problems including surface roughness effect. They combined Hirs bulk flow concept with formulated resistance law and derived the generalized turbulent lubrication equation including the surface roughness. Hashimoto [38] studied the effects of "O-Type" cavitation on the static and dynamic characteristics of turbulent journal bearing submerged in the low viscosity lubricant. He expanded an idea of general short bearing theory proposed by Pan to submerged turbulent journal bearings, "O-type" cavitation pattern, load carrying capacity and attitude angle are determined for a wide range of eccentricity ratio in both laminar and turbulent flow cases. Kumar and Mishra [39] presented steady state analysis of non-circular worn journal bearings in non-laminar lubrication regimes. They computed and obtained results compared with published results. They observed that geometric change caused by wear has a significant effect on the steady state characteristics of bearing. Andres [40] considered fluid inertia effects on turbulent hybrid journal bearings. His analysis includes the effects of recess on fluid compressibility and a model for pressure rise within the recessed region. Yu and Szeri [41] studied performance of partial journal bearing in laminar regime. They presented an approximate numerical method for

carried out study on the performance of worn non-recessed hole-entry hybrid journal bearing system. The results of bearing performance characteristics parameters in terms of maximum fluid-film pressure, minimum fluid-film thickness, flow rate and stability threshold speed, etc have been presented. The results indicate that the wear affect the bearing performance considerably. Ives and Rowe [15] carried their work on theoretical investigation of slot-entry hybrid journal bearing operating in super laminar flow regime. Their work consist the effect of super laminar flow on the optimization of slot-entry hybrid journal bearing system. They concluded that the main effect of operating in the super laminar flow regions on bearings performance was to greatly prediction of friction power. Constantinescu [16] analyzed theoretically three dimensional motions in the lubricant layer by using Prandtl's mixing length theory. He presented calculations for journal and thrust bearings subjected to turbulent lubrication. Constantinescu [17] studied the transient conditions from laminar to turbulent regime for gas lubricated bearings. He developed a method to determine the pressure and the operating characteristics for a high bearing number. From the results, he showed that turbulence does not alter quantitatively the operating conditions of gas lubricated bearings. Constantinescu and Galetuse [18] developed mixing length theory for determining the velocity profile and pressure distribution in turbulent fluid film, later same theory used for determining the friction stresses. They also used same formula for calculation of the friction forces and friction torques in journal bearings and slider bearings. Constantinescu [19] analyzed and come on the conclusion that thermal effects are in general less important in turbulent flow as compared to laminar and he found that all the methods studied by him, can be extended in order to evaluate the operating characteristics of fluid film bearing in transition region between laminar and fully developed turbulent flow. Constantinescu and Galetuse [20] assumed the shape of the velocity profiles is not strongly affected by inertia forces and evaluated the momentum equations for laminar and turbulent flow in fluid film bearings. Galetuse [21] performed experiments concern the turbulent motion of an air film between a rotating cylindrical surface and a fixed plane surface. From the experiments he determined the pressure distribution for the main flow direction and the lateral direction. He gave the important information regarding effect of inertia forces when the lubricant film thickness shows large variation. Constantinescu and Galetuse [22] presented data for operating characteristics of journal bearings operating in turbulent inertial flow. They found that, at least for the range of variation of the Reynolds number and the clearance ratio which might

occur in practical applications and the influence of the inertia forces is still small. Ng and Pan [23] presented a linearized turbulent lubrication theory by utilizing the Reichardt's formula of eddy viscosity. They utilized the concept of eddy viscosity to represent the turbulent stresses in term of mean velocity gradient. Elrod [24] derived and illustrated some general relations for the behavior of thin lubricating films in the presence of roughness. He suggested a smoother form of Reynolds's equation in which appears certain flow factors to be determined by statistical computations. He used Fourier transform for computing problem. After the Constantinescu and Ng, Pan and Elrod a new theory has been developed by Hirs [25]. This theory based on bulk flow approach which requires no physical representation of the turbulent transport mechanism. A particular advantage of the approach is that empirical constants used in the theory can be derived from the bulk flow measurement without the determination of velocity profiles. He provided a theoretical basis for the design of bearings lubricated by fluids of low kinematic viscosity. Hirs [26] verified turbulent film flow theories based on number of experimental results available in the literature and showed that the theory to be compatible with these results. He set up a classification system for turbulent film flow experiments. Burton [27] gave approximations in turbulent film analysis. He presented the relationship between flow and wall stress. He considered the effects of inertia at steps and also effect of roughness. Burton and Hsu [28] analyzed the integrated form of the momentum and continuity equations, supported by velocity profile measurement on crossed Couette and Pressure flows. They discussed the contribution of inertia with regard to an experimentally and analytically predicted static instability under small displacement from the central position of shaft. Taylor and Dowson [29] presented review of the existing turbulent lubrication theories. They discussed the differences between them and limitations of the alternative approaches. They also represented the basic concept which deals with in an appropriate manner in order to give the designer a feel of the nature of problem. Kumar [30] studied non-laminar behavior in bearings and presented with the emphasis on those aspects which are concerned with the performance of journal bearing under turbulent film operation. He described analytical and relevant experimental studies and compared the advantages and limitations. Kumar [31] studied plain hydrodynamic bearing in the turbulent regime and presented a critical review on journal bearings operating in the turbulent regime. Kumar [32] determined the condition of dynamic stability of hydro-dynamically lubricated plain circular bearings of finite length with turbulent flow. He analyzed dynamic stability with the help

of Routh-Hurwitz criterion by using the perturbation technique. Vohr and Mein-kai Ho [33] presented a turbulent energy model for determination of turbulent stresses is used to calculate velocity profiles in lubricant films. They showed that the results are matched with prediction of the previously established turbulent lubrication theory given by Elrod, Ng and Pan. Vohr et al. [34] discussed an analytical and experimental investigation of turbulent flow in bearing films including the effects of convective fluid inertia forces. They analyzed turbulence is treated by means of turbulent viscosity correction factor. They studied the pad bearings of arbitrary surface geometry by using a computer program to calculate the film pressure developed in such bearings. They found that good match between results. Hashimoto and Wada [35] studied turbulent lubrication of tilting-pad thrust bearings with the effect of thermal and elastic deformations. They introduced the effect of pad deformations when analyzing performances of such bearings running in the turbulent condition. Hashimoto et al. [36] worked on application of short bearing and presented theory to dynamic characteristics problem related to turbulent journal bearings. They found that the turbulence has significant effect on the dynamic behavior of rotor bearing system and the short bearing theory has an advantage of less computational time required for the calculation for the journal centre trajectories with an acceptable accuracy. Hashimoto and Wada [37] presented theoretical approach to turbulent lubrication problems including surface roughness effect. They combined Hirs bulk flow concept with formulated resistance law and derived the generalized turbulent lubrication equation including the surface roughness. Hashimoto [38] studied the effects of "O-Type" cavitation on the static and dynamic characteristics of turbulent journal bearing submerged in the low viscosity lubricant. He expanded an idea of general short bearing theory proposed by Pan to submerged turbulent journal bearings, "O-type" cavitation pattern, load carrying capacity and attitude angle are determined for a wide range of eccentricity ratio in both laminar and turbulent flow cases. Kumar and Mishra [39] presented steady state analysis of non-circular worn journal bearings in non-laminar lubrication regimes. They computed and obtained results compared with published results. They observed that geometric change caused by wear has a significant effect on the steady state characteristics of bearing. Andres [40] considered fluid inertia effects on turbulent hybrid journal bearings. His analysis includes the effects of recess on fluid compressibility and a model for pressure rise within the recessed region. Yu and Szeri [41] studied performance of partial journal bearing in laminar regime. They presented an approximate numerical method for

solving the thermodynamic problem in journal bearings. Wilcock and Pinkus [42] consider the effect of turbulence and viscosity variation on the dynamic stiffness and damping coefficients of fluid film journal bearings. Tieu and Kosasih [43] studied a transition turbulent lubrication theory considering mixing length concept. They presented that the Reynolds stress model using the mixing length expression is able to account for the effect of local shear stress gradient and it can be extended to apply in the transition region. Chun and Ha [44] presented study on mixing flow effects in a high-speed journal bearing. They studied the behavior of a high-speed journal bearing generating turbulent motion, it is found that in mixing condition and the convective boundary condition cannot be substituted by the adiabatic boundary condition for the design purpose of journal bearings. They presented wall temperature has no effect on load and friction and most dominant factor for frictional loss for turbulent conditions is the high shaft speed. Frene et al. [45] studied combined thin-film and Navier–Stokes analysis for higher value of Reynolds number in lubrication. They presented effects of inertia forces in laminar and in turbulent flows and results obtained. The complete Navier Stokes equation has been presented and described how they are included in the classic lubrication theory. Jian and Chen [46] worked on bifurcation and chaos analysis of a flexible rotor supported by turbulent long journal bearing system. They presented the prediction stability of the rotor–bearing system and the undesirable behavior of the rotor and bearing center can be avoided. Shenoy and Pai [47] investigate the performance of an externally adjustable fluid-film bearing including misalignment and turbulence effects. They studied the effect of turbulence and misalignment on steady state characteristics of a centrally loaded single pad externally adjustable bearing. They also found that Reynolds equation incorporated with linearized turbulent lubrication model of Ng and Pan is solved using a finite difference method. Nicodemus and Sharma [48] deals with the influence of wear on the performance of a capillary-compensated four-pocket hybrid journal bearing system operating in a turbulent regime by considering various geometric shapes of recess. They concluded that the direct fluid film stiffness coefficients get reduced significantly when bearings operate in a turbulent regime as compared with the bearings operate in laminar regime. Dufrane et al. [49] investigated the worn journal bearings used in steam turbine generators and established a model of wear geometry for the analysis of journal bearings. They subsequently analyzed the effects of geometric change due to wear on bearing lubrication at low operating speeds. Duckworth and Forrester [50] has been studied experimentally, the wear in plain hydrodynamic journal bearings

under repeated cycles of starting and stopping operations. They observed, wear occurred due to localized changes in diametral clearance, surface finish, and roundness of the bearing's bore and these changes were measured after various numbers of operating cycles had been completed. Forrester [51] studied the influence of wear on the performance of journal bearings. They analyzed quantitatively and qualitatively several damages in the bearings to examine the modes of bearing failure due to wear. Hashimoto et al. [52] presented the steady state characteristics of worn journal bearings operating in both laminar and turbulent regimes. They concluded that the pressure distributions significantly increase at high eccentricity ratio in turbulent regime. Vaidyanathan and Keith [53] studied the worn journal bearings and considered the effect of cavitation on the performance behavior of pressure distribution, eccentricity ratio, Sommerfeld number and attitude angle. Jain et al. [54] deals with the performance of a multi recess flexible journal bearing using various flow control devices namely capillary, constant flow valve, orifice and membrane restrictors for hydrostatic as well as hybrid modes of operations. They used Finite Element Method for solving the governing equations. They concluded from the computed results that the proper selection of the type of restrictor with the value of deformation coefficient ($\bar{C}_d$) is essential in order to improve bearing performance. Kumar and Rao [55] investigated theoretically the steady state performance of finite hydrodynamic porous journal bearings in turbulent regime using Constantinescu's turbulent lubrication theory. They studied the effect of turbulence on eccentricity ratio, slenderness ratio on the load carrying capacity, friction coefficient and oil flow rate. Kumar and Mishra [56] presented steady state analysis of non-circular worn journal bearings in non-laminar lubrication regimes. Fillon and Bouyer [57] conducted a thermo hydrodynamic study related to worn journal bearing system, and analyzed the effect of wear on bearing characteristics which includes pressure and fluid film thickness distribution, eccentricity ratio, attitude angle, minimum fluid film thickness and temperature for different speed and load .They observed significant reduction in the temperature distribution of the fluid film due to tendency of the bearing to go in to the cavity formed by wear. Papadopoulos et al. [58] studied the significance of wear on the surface of bearings, which support rotating shafts for long periods of time. They studied modeled rotor by using the finite element method with 4DOF's per node, including the gyroscopic effect. The dynamic coefficients of the bearing are calculated by solving the Reynolds equation, thus obtaining the pressure distribution of the oil film, and by finding the equilibrium position. They presented theoretical work on this

particular problem and verified it experimentally. They concluded that the stability of the system as a function of both rotational speed and wear. Gertzos et al. [59] presented study of bearing characteristics such as eccentricity, attitude angle, lubricant flow and friction coefficient versus Sommerfeld number for various wear depths. They solved the Navier–Stokes equations by using Computational Fluid Dynamics (CFD) analysis. Soni et al. [60] studied the Navier-Stokes equation by using the non-linear theory proposed by Elrod and Ng, and solved numerically for the flow field in the clearance space of a journal bearing. They presented the performance characteristics of a finite circular hydrodynamic bearing (aspect ratio $L/D = 1$) in terms of the Sommerfeld number, attitude angle, oil flow, friction coefficient and temperature rise parameter at various eccentricities for Reynolds numbers up to 13300.

2.4 GAP IN THE LITERATURE

A through scan of the literature survey reveals that very limited information is available in the area of the analysis of non-recessed hole-entry hybrid journal bearing system operates in turbulent regime. To the best knowledge of the author, no such study has been reported for the performance of a constant flow valve compensated non-recessed hole-entry hybrid journal bearing system operates in turbulent regime. Further, in recent years several studies have been reported in open literature that addresses the issue of wear in fluid film bearings. The wear in the bearings is primarily caused due to numerous start/stop operations during the life span of the machine. These studies clearly demonstrate that the wear greatly affects the bearing performance. Therefore, for realistic prediction of bearing performance, the influence of wear is essential to be considered in the analysis. Thus the present work has been planed to bridge this gap in the literature.

CHAPTER-3 ANALYSES

In this chapter, hybrid journal bearing system operating in turbulent regime is analyzed by considering the solution of the Reynolds equation governing the flow of lubricant in the bearing clearance space including flow through the restrictor as a constraint. The simultaneous solution of these equations yields pressure distribution in the clearance space of the bearing. After the pressure distribution is established, the static and dynamic performance characteristics of bearing are computed.

In the following sections, the mathematical model of Reynolds equation has been obtained theoretically and the Reynolds equation has been solved by using Constantinescu's [16,19] turbulent lubrication model.

3.1 ANALYTICAL FORMULATION

The following section describes the relevant equations to be used for the analysis of fluid-film bearing system operates turbulent regime.

3.1.1 NOMINAL FLUID-FILM THICKNESS

The nominal fluid-film thickness for unworn journal bearing is related to the geometry of the film which is dependent on the steady state journal centre position X_J and Z_J for finite journal bearing system is described as [7].

$$\overline{h}_0 = 1 - \overline{X}_J \cos\alpha - \overline{Z}_J \sin\alpha \tag{3.1}$$

3.1.2 THE EFFECT OF WEAR ON BEARING GEOMETRY

The geometry of the worn zone is shown schematically in Fig. 3.1. Dufrane et al. [49] assumed an abrasive wear model with the worn arc at a radius larger than the radius of the journal. Based on the visual observation, they stated that the shaft axis is symmetrical at the bottom of the bearing and the wear pattern is uniform along the length of bearing.

Following is expression for nominal fluid film thickness for a worn journal bearing.

$$\overline{h} = \overline{h}_0 + \partial\overline{h} = 1 - \overline{X}_J \cos\alpha - \overline{Z}_J \sin\alpha + \partial\overline{h} \tag{3.2}$$

The wear defect value $\partial\bar{h}$ is added to the nominal fluid film thickness.

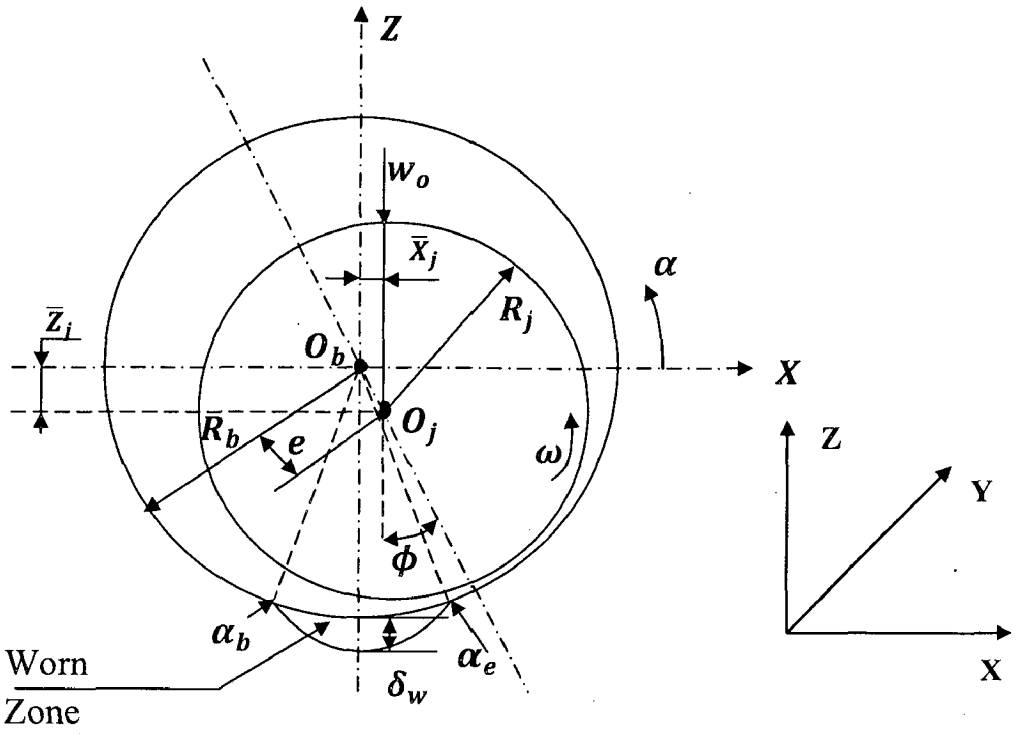

Fig. 3.1 Geometrical presentation of worn bearing [49]

$$\partial\bar{h} = \bar{\delta}_w - 1 - sin\alpha \;\; ; \;\; \text{for } \alpha_b \leq \alpha \leq \alpha_e \tag{3.3}$$

$$\partial\bar{h} = 0 \; ; \;\; \text{for } \alpha < \alpha_b \text{ or } \alpha > \alpha_e \tag{3.4}$$

The angles α_b and α_e are at the beginning and end of the footprint respectively and their values are computed by putting Eq. (3.4) into Eq. (3.3), i.e.

$$sin\alpha = \bar{\delta}_w - 1 \tag{3.5}$$

3.2 FLOW FIELD EQUATION

The dimensional Reynolds equation which governs the fluid flow in the clearance space of journal and bearing can be written as equation (3.1) with the following assumptions:

(i) The lubricant in the clearance space is an incompressible, isoviscous and Newtonian.

(ii) Body forces and fluid inertia is neglected.

(iii) The viscosity is constant throughout the fluid film thickness.

The equation is solved using finite element (FEM) for the computation of pressure in both laminar and turbulent flow regime as [48]

$$\frac{\partial}{\partial\alpha}\left[\frac{h^3}{G_\alpha\mu}\frac{\partial p}{\partial\alpha}\right]+\frac{\partial}{\partial\beta}\left[\frac{h^3}{G_\beta\mu}\frac{\partial p}{\partial\beta}\right]=\frac{U}{2}\frac{\partial h}{\partial\alpha}+\frac{\partial h}{\partial\tau} \tag{3.6}$$

Where, $\bar{h}$ is given by Eq. (3.2) and the turbulent coefficients G_α and G_β are functions of local Reynolds number (R_e^*) and expression given by Constantinescu et al. [19] are

$$G_\alpha = 12+0.026(\mathrm{R^*_e})^{0.8265} \tag{3.7}$$

$$G_\beta = 12+0.0198(\mathrm{R^*_e})^{0.741} \tag{3.8}$$

Introducing the non-dimensional parameters in the equation (3.6) and equation (3.6) reduces to the following non-dimensional form as [48]

$$\frac{\partial}{\partial\alpha}\left[\frac{\bar{h}^3}{G_\alpha\bar{\mu}}\frac{\partial\bar{p}}{\partial\alpha}\right]+\frac{\partial}{\partial\beta}\left[\frac{\bar{h}^3}{G_\beta\bar{\mu}}\frac{\partial\bar{p}}{\partial\beta}\right]=\frac{\Omega}{2}\frac{\partial\bar{h}}{\partial\alpha}+\frac{\partial\bar{h}}{\partial\tau} \tag{3.9}$$

3.3 FINITE ELEMENT FORMULATION

Using the finite element formulation and Galerkin's technique the equation (3.9) reduces to following form

$$\int_{A^e}\int\left[\left[\frac{\partial}{\partial\alpha}\left[\frac{\bar{h}^3}{G_\alpha\bar{\mu}}\frac{\partial\bar{p}}{\partial\alpha}\right]+\frac{\partial}{\partial\beta}\left[\frac{\bar{h}^3}{G_\beta\bar{\mu}}\frac{\partial\bar{p}}{\partial\beta}\right]-\frac{\Omega}{2}\frac{\partial\bar{h}}{\partial\alpha}-\frac{\partial\bar{h}}{\partial\tau}\right]\right]N_i d\alpha d\beta=0 \tag{3.10}$$

A^e= Area of element

Integrating equation (3.10) part wise and simplifying it, we get

$$\int_{A^e}\int\frac{\bar{h}^3}{\bar{\mu}}\left[\frac{1}{G_\alpha}\frac{\partial N_i}{\partial\alpha}\frac{\partial\bar{p}}{\partial\alpha}+\frac{1}{G_\beta}\frac{\partial N_i}{\partial\beta}\frac{\partial\bar{p}}{\partial\beta}\right]d\alpha d\beta-\int_{A^e}\int-\frac{\Omega}{2}\bar{h}\frac{\partial N_i}{\partial\alpha}\,d\alpha d\beta-\int_{A^e}\int\frac{\partial h}{\partial\tau}d\alpha d\beta-$$

$$\int_{\Gamma^e}\frac{\bar{h}^3}{G_\alpha\bar{\mu}}N_i\frac{\partial\bar{p}}{\partial\alpha}d\Gamma-\int_{\Gamma^e}\frac{\bar{h}^3}{G_\beta\bar{\mu}}N_i\frac{\partial\bar{p}}{\partial\beta}d\Gamma+\int_{\Gamma^e}\frac{\Omega}{2}\bar{h}N_i d\Gamma=0 \tag{3.11}$$

The fluid flow is discretized using 4-noded quadrilateral isoparametric elements. The pressure is considered to be distributed linearly over an element and is expressed as

$$\bar{p}=\sum_{i=1}^{4}N_i\bar{p}_i, \tag{3.12}$$

Where N_i is the shape function for an element and in terms of local co-ordinates are given as:

$$\left.\begin{aligned} N_1 &= \tfrac{1}{4}(1-\xi)(1-\eta) \\ N_2 &= \tfrac{1}{4}(1+\xi)(1-\eta) \\ N_3 &= \tfrac{1}{4}(1+\xi)(1+\eta) \\ N_4 &= \tfrac{1}{4}(1-\xi)(1+\eta) \end{aligned}\right\} \tag{3.13}$$

$$\overline{p}^e = [N_1, N_2, N_3, N_4] \begin{Bmatrix} \overline{p}_1 \\ \overline{p}_2 \\ \overline{p}_3 \\ \overline{p}_4 \end{Bmatrix} \tag{3.14}$$

Differentiating the above equation with respect to α and β respectively, given the following expressions

$$\left.\begin{aligned} \frac{\partial \overline{p}^e}{\partial \alpha} &= \begin{bmatrix} \frac{\partial N_1}{\partial \alpha} & \frac{\partial N_2}{\partial \alpha} & \frac{\partial N_3}{\partial \alpha} & \frac{\partial N_4}{\partial \alpha} \end{bmatrix} \begin{Bmatrix} \overline{p}_1 \\ \overline{p}_2 \\ \overline{p}_3 \\ \overline{p}_4 \end{Bmatrix} \\ \frac{\partial \overline{p}^e}{\partial \beta} &= \begin{bmatrix} \frac{\partial N_1}{\partial \beta} & \frac{\partial N_2}{\partial \beta} & \frac{\partial N_3}{\partial \beta} & \frac{\partial N_4}{\partial \beta} \end{bmatrix} \begin{Bmatrix} \overline{p}_1 \\ \overline{p}_2 \\ \overline{p}_3 \\ \overline{p}_4 \end{Bmatrix} \end{aligned}\right\} \tag{3.15}$$

After substituting the above expressions in the equation (3.11) we get

$$\int_{A^e} \int \frac{\overline{h}^3}{\overline{\mu}} \left[\left[\frac{1}{G_\alpha} \frac{\partial N_i}{\partial \alpha} \frac{\partial N_1}{\partial \alpha} + \frac{1}{G_\beta} \frac{\partial N_i}{\partial \beta} \frac{\partial N_1}{\partial \beta} \right] \overline{p}_1 + \left[\frac{\partial N_i}{\partial \alpha} \frac{\partial N_2}{\partial \alpha} + \frac{\partial N_i}{\partial \beta} \frac{\partial N_2}{\partial \beta} \right] \overline{p}_2 + \left[\frac{\partial N_i}{\partial \alpha} \frac{\partial N_3}{\partial \alpha} + \frac{\partial N_i}{\partial \beta} \frac{\partial N_3}{\partial \beta} \right] \overline{p}_3 + \left[\frac{\partial N_i}{\partial \alpha} \frac{\partial N_4}{\partial \alpha} + \frac{\partial N_i}{\partial \beta} \frac{\partial N_4}{\partial \beta} \right] \overline{p}_4 \right] d\alpha d\beta - \frac{\Omega}{2} \int_{A^e} \int \overline{h} \frac{\partial N_i}{\partial \alpha} \, d\alpha \, d\beta - \int_{A^e} \int \frac{\partial \overline{h}}{\partial \tau} \, d\alpha d\beta - \int N_i \frac{\overline{h}^3}{\overline{\mu}} \left[\frac{1}{G_\alpha} \frac{\partial \overline{p}}{\partial \alpha} + \frac{1}{G_\beta} \frac{\partial \overline{p}}{\partial \beta} \right] d\tau + \int_{\tau^e} N_i \frac{\overline{h}}{2} \Omega \, d\Gamma = 0 \tag{3.16}$$

Representing the above expression in the matrix form as follows:

$$[\overline{F}]^e \{\overline{p}\}^e = \{\overline{Q}\}^e + \Omega \{\overline{R_H}\}^e + \dot{\overline{X}}_j \{\overline{R}_{xj}\}^e + \dot{\overline{Z}}_j \{\overline{R}_{zj}\}^e \tag{3.17}$$

where,

$$\overline{F}_{ij}^{e} = \int_{A^e} \int \frac{\overline{h}^3}{\overline{\mu}} \left[\frac{1}{G_\alpha} \frac{\partial N_i}{\partial \alpha} \frac{\partial N_j}{\partial \alpha} + \frac{1}{G_\beta} \frac{\partial N_i}{\partial \beta} \frac{\partial N_j}{\partial \beta} \right] d\alpha d\beta$$

$$= \int_{-1}^{+1} \int_{-1}^{+1} \frac{\overline{h}^3}{\overline{\mu}} \left[\frac{1}{G_\alpha} \frac{\partial N_i}{\partial \alpha} \frac{\partial N_j}{\partial \alpha} + \frac{1}{G_\beta} \frac{\partial N_i}{\partial \beta} \frac{\partial N_j}{\partial \beta} \right] |\overline{J}_L| d\xi \, d\eta$$

$$\overline{R}_{Hj}^{e} = \int_{A^e} \int \frac{\overline{h}}{2} \frac{\partial N_i}{\partial \alpha} \, d\alpha d\beta = \int_{-1}^{+1} \int_{-1}^{+1} \frac{\overline{h}}{2} \frac{\partial N_i}{\partial \alpha} |\overline{J}_L| \, d\xi \, d\eta$$

$$\overline{R}_{xij}^{e} = \int_{A^e} \int N_i \cos\alpha \, d\alpha d\beta = \int_{-1}^{+1} \int_{-1}^{+1} N_i \cos\alpha \, |\overline{J}_L| \, d\xi \, d\eta$$

$$\overline{R}_{Zij}^{e} = \int_{A^e} \int N_i \sin\alpha \, d\alpha d\beta = \int_{-1}^{+1} \int_{-1}^{+1} N_i \sin\alpha \, |\overline{J}_L| \, d\xi \, d\eta$$

$$\overline{Q}_j^{e} = \int_{\tau^e} \frac{\overline{h}^3}{\overline{\mu}} \left[\frac{1}{G_\alpha} \frac{\partial \overline{p}}{\partial \alpha} + \frac{1}{G_\beta} \frac{\partial \overline{p}}{\partial \beta} \right] N_i d\tau - \frac{\Omega}{2} \int \overline{h} \, N_i d\tau$$

$$= -\frac{\Omega}{2} \int_{-1}^{+1} \overline{h} \, N_i \, |\overline{J}_{L2}| d\eta + \int_{-1}^{+1} \frac{\overline{h}^3}{\overline{\mu}} \frac{1}{G_\alpha} \frac{\partial \overline{p}}{\partial \alpha} N_i |\overline{J}_{L2}| \, d\eta + \int_{-1}^{+1} \frac{\overline{h}^3}{\overline{\mu}} \frac{1}{G_\beta} \frac{\partial \overline{p}}{\partial \beta} N_i |\overline{J}_{L1}| \, d\xi \qquad (3.18)$$

$(i, j = 1,2,3,4)$

After assembling of all the elements of the discretized flow-field, the system equation is obtained as;

$$[\overline{F}] \{\overline{p}\} = \{\overline{Q}\} + \Omega \{\overline{R}_H\} + \dot{\overline{X}}_j \{\overline{R}_{xj}\} + \dot{\overline{Z}}_j \{\overline{R}_{zj}\} \qquad (3.19)$$

where,

$$|\overline{J}_L| = \begin{vmatrix} \frac{\partial \alpha}{\partial \xi} & \frac{\partial \beta}{\partial \xi} \\ \frac{\partial \alpha}{\partial \eta} & \frac{\partial \beta}{\partial \eta} \end{vmatrix}, \quad |\overline{J}_{L1}| = \left| \frac{\partial \alpha}{\partial \xi} \right|, \quad |\overline{J}_{L2}| = \left| \frac{\partial \beta}{\partial \eta} \right|$$

3.4 EQUATION OF FLOW THROUGH RESTRICTORS

The flow of lubricant through different flow controlling devices is given by the following non-dimensional equations as [54]

1. **Equation of flow through constant flow valve restrictor**

$$\overline{Q}_R = \overline{Q}_c \qquad (3.20a)$$

where, $\overline{Q}_c = Q \left(\frac{\mu_r}{c^3 p_s} \right)$

2. Equation of flow through Capillary restrictor

$$\overline{Q}_R = \overline{C}_{s2}\left(1 - \overline{p}_c\right) \tag{3.20b}$$

where, $\overline{C}_{s2} = \left(\frac{\pi r_c^4}{8c^3 l_c}\right)$

3. Equation of flow through Orifice restrictor

$$\overline{Q}_R = \overline{C}_{s2}\left(1 - \overline{p}_c\right)^{1/2} \tag{3.20c}$$

where, $\overline{C}_{s2} = \left\{\frac{3\pi d_o^2 \mu_r \psi_d}{c^3}\right\}\left(\frac{2}{\rho p_s}\right)^{1/2}$

3.5 BOUNDARY CONDITIONS

Boundary conditions relevant to the lubricant flow field are as follows:

(i) At the external boundary, nodal pressures are zero; i.e. $\overline{p}|_{\beta=\mp 1.0} = 0.0$.

(ii) Nodal pressures for the nodes appearing on the hole boundary are equal.

(iii) Nodal flow is Zero at every internal node excluding the nodes appearing on the hole and external boundaries.

(iv) At the trailing edge of positive region, the Reynolds boundary condition is applied; i.e. $\bar{p} = \frac{\partial \bar{p}}{\partial \alpha} = 0.0$.

Journal Centre Equilibrium Position

In the static equilibrium position of the journal bearing system$(\overline{X}_J, \overline{Z}_J)$, the fluid films forces are balanced by external forces acting on the journal. For a given external load, tentative values of journal centre co-ordinates are used as input.

After expanding the fluid film reaction components $\overline{F}_x$ and $\overline{F}_z$ by Taylor's series and considering the first order terms only, the correction $(\Delta\overline{X}_j|_i, \Delta\overline{Z}_j|_i)$ on the journal centre co-ordinates is obtained as

$$\Delta\overline{X}_j|_i = \frac{-1}{D_j}\left[\frac{\partial\overline{F}_z}{\partial\overline{Z}_j}\Big|_i - \frac{\partial\overline{F}_x}{\partial\overline{Z}_j}\Big|_i\right]\begin{Bmatrix}\overline{F}_x|_i \\ \overline{F}_z|_i - \overline{W}_o\end{Bmatrix}$$

$$\Delta\overline{Z}_j|_i = \frac{-1}{D_j}\left[\frac{\partial\overline{F}_z}{\partial\overline{X}_j}\Big|_i - \frac{\partial\overline{F}_x}{\partial\overline{X}_j}\Big|_i\right]\begin{Bmatrix}\overline{F}_x|_i \\ \overline{F}_z|_i - \overline{W}_o\end{Bmatrix} \tag{3.21}$$

The new journal centre position co-ordinates are expressed as

$$\bar{X}_j\big|_{i+1} = \bar{X}_j\big|_i + \Delta\bar{X}_j\big|_i$$

$$\bar{Z}_j\big|_{i+1} = \bar{Z}_j\big|_i + \Delta\bar{Z}_j\big|_i \qquad (3.22)$$

Where,

$$\bar{D}_j = \left[\frac{\partial\bar{F}_z}{\partial\bar{X}_j}\Big|_i \frac{\partial\bar{F}_z}{\partial\bar{Z}_j}\Big|_i - \frac{\partial\bar{F}_x}{\partial\bar{Z}_j}\Big|_i \frac{\partial\bar{F}_x}{\partial\bar{X}_j}\Big|_i\right]$$

The final journal equilibrium position is established using an iterative scheme.

3.6 PERFORMANCE CHARACTERISTICS

To study the behavior of hole-entry hybrid journal bearing, its static as well as dynamic characteristics are to be known. The static performance characteristics include load carrying capacity, minimum film thickness, bearing flow and attitude angle. The dynamic performance characteristics include stiffness coefficients, damping coefficients, and threshold speed. The expression for static and dynamic performance characteristics of hybrid journal bearings are given in the following sections.

3.6.1 STATIC PERFORMANCE CHARACTERISTICS

To compute the static performance characteristics, for steady state condition the velocity terms are taken zero ($\dot{\bar{X}}_j = \dot{\bar{Z}}_j = 0.0$) on the right hand side of the system equation (3.19). Then the system equation will be modified as

$$[\bar{F}]\{\bar{p}\} = \{\bar{Q}\} + \Omega\{\bar{R}_H\} \qquad (3.23)$$

The nodal pressures are computed by applying suitable boundary conditions to the equation (3.23). After computing the nodal pressures the static performance characteristics are computed using the following expressions.

Load Carrying Capacity ($\bar{W}_o$)

The fluid film pressure obtained from the Reynolds equation is integrated to obtain the fluid film reaction components along and perpendicular to the line of centers as follows:

$$\left.\begin{aligned}\bar{F}_x &= -\int_{-\lambda}^{+\lambda}\int_0^{2\pi}\bar{p}\cos\alpha\, d\alpha\, d\beta \\ \bar{F}_z &= -\int_{-\lambda}^{+\lambda}\int_0^{2\pi}\bar{p}\sin\alpha\, d\alpha\, d\beta\end{aligned}\right\} \quad (3.24)$$

The resulting fluid film reaction is given by

$$\bar{F} = \left[\bar{F}_x^{\,2} + \bar{F}_z^{\,2}\right]^{1/2} \quad (3.25)$$

3.6.2 DYNAMIC PERFORMANCE CHARACTERISTICS

The stiffness and damping coefficients determines the dynamic performance of journal bearing, when the journal is disturbed from its static equilibrium position. The eight stiffness and damping coefficients are computed using the following expressions.

Fluid Film Stiffness Coefficients $(\bar{S}_{mn})$

The negative rate of change in fluid film reaction with respect to film thickness is defined as the fluid film stiffness.

$$\bar{S}_{mn} = -\frac{\partial \bar{F}_m}{\partial \bar{X}_n} \qquad (m, n = 1,2)$$

m = direction of force

n = direction of displacement

In the matrix form

$$\begin{bmatrix}\bar{S}_{11} & \bar{S}_{12} \\ \bar{S}_{21} & \bar{S}_{22}\end{bmatrix} = -\begin{bmatrix}\frac{\partial \bar{F}_x}{\partial \bar{X}_j} & \frac{\partial \bar{F}_x}{\partial \bar{Z}_j} \\ \frac{\partial \bar{F}_z}{\partial \bar{X}_j} & \frac{\partial \bar{F}_z}{\partial \bar{Z}_j}\end{bmatrix} \quad (3.26)$$

Fluid Film Damping Coefficient $(\bar{C}_{mn})$

The negative rate of change in fluid film reaction with respect to journal centre velocities is defined as fluid film damping coefficients.

$$\bar{C}_{mn} = -\frac{\partial \bar{F}_m}{\partial \dot{\bar{X}}_n} \qquad (m, n = 1, 2)$$

In the matrix form

$$\begin{bmatrix}\bar{C}_{11} & \bar{C}_{12} \\ \bar{C}_{21} & \bar{C}_{22}\end{bmatrix} = -\begin{bmatrix}\frac{\partial \bar{F}_X}{\partial \dot{\bar{X}}_j} & \frac{\partial \bar{F}_X}{\partial \dot{\bar{Z}}_j} \\ \frac{\partial \bar{F}_Z}{\partial \dot{\bar{X}}_j} & \frac{\partial \bar{F}_Z}{\partial \dot{\bar{Z}}_j}\end{bmatrix} \quad (3.27)$$

3.7 LINEARIZED EQUATION OF MOTION

With in the neighborhood of the equilibrium position, the restoring fluid film force components on the journal can be regarded as linear functions of displacement and velocity vectors.

The linearized equation of motion of the journal for the lateral motion can be derived in the following non-dimensional from.

$$[\overline{M}]\{\ddot{\overline{X}}\} + [\overline{C}]\{\dot{\overline{X}}\} + [\overline{S}]\{\overline{X}\} = 0 \tag{3.28}$$

In matrix from the equation of motion is written as:

$$\begin{bmatrix} \overline{M}_j & 0 \\ 0 & \overline{M}_j \end{bmatrix} \begin{Bmatrix} \ddot{\overline{X}}_j \\ \ddot{\overline{Z}}_j \end{Bmatrix} + \begin{bmatrix} \overline{C}_{11} & \overline{C}_{12} \\ \overline{C}_{21} & \overline{C}_{22} \end{bmatrix} \begin{Bmatrix} \dot{\overline{X}}_j \\ \dot{\overline{Z}}_j \end{Bmatrix} + \begin{bmatrix} \overline{S}_{11} & \overline{S}_{12} \\ \overline{S}_{21} & \overline{S}_{22} \end{bmatrix} \begin{Bmatrix} \overline{X}_j \\ \overline{Z}_j \end{Bmatrix} = \begin{Bmatrix} 0 \\ 0 \end{Bmatrix} \tag{3.29}$$

3.8 STABILITY OF THE LINEARIZED SYSTEM

The stability of the journal bearing system determined by applying Routh's Criteria to the characteristics equation of free vibration linearized equation of motion.

$$[\overline{M}]\{\ddot{\overline{X}}\} + [\overline{C}]\{\dot{\overline{X}}\} + [\overline{S}]\{\overline{X}\} = 0$$

The characteristics equation is

$$a_1 s^4 + a_2 s^3 + a_3 s^2 + a_4 s^1 + a_5 = 0$$

S = complex variable

The necessary conditions are

$$\left.\begin{aligned} a_1 &= 1 && > 0 \\ a_2 &= \frac{1}{\overline{M}_j}\left[\overline{C}_{11} + \overline{C}_{22}\right] && > 0 \\ a_3 &= \frac{1}{\overline{M}_j^2}\left[\overline{C}_{11}\overline{C}_{22} + \overline{M}_j\left[\overline{S}_{11} + \overline{S}_{22}\right] - \overline{C}_{12}\overline{C}_{21}\right] && > 0 \\ a_4 &= \frac{1}{\overline{M}_j^2}\left[\overline{S}_{11}\overline{C}_{22} + \overline{S}_{22}\overline{C}_{11} - \left[\overline{S}_{12}\overline{C}_{21} + \overline{S}_{21}\overline{C}_{12}\right]\right] && > 0 \\ a_5 &= \frac{1}{\overline{M}_j^2}\left[\overline{S}_{11}\overline{S}_{22} - \overline{S}_{12}\overline{S}_{21}\right] && > 0 \end{aligned}\right\} \tag{3.30}$$

Sufficiently condition (by Routh's Criteria) for stability is,

$$a_2\, a_3 - a_4 > 0$$

$$a_2\, a_3 a_4 - (a_4)^2 - (a_2)^2 - a_5 > 0 \tag{3.31}$$

The non-dimensional critical mass ($\overline{M}_c$) of the journal can be found from (3.30) and (3.31).

Threshold speed of journal at the threshold of instability is given by

$$\overline{\omega}_{th} = \left[\frac{\overline{M}_c}{\overline{F}_o}\right]^{1/2} \tag{3.32}$$

Where

$\overline{M}_c$ = Critical journal mass = $\frac{\overline{G}_1}{\overline{G}_2 - \overline{G}_3}$

$\overline{F}_o$ = Resultant fluid film force or reaction

$$\overline{G}_1 = [\overline{C}_{11}\,\overline{C}_{22} - \overline{C}_{21}\overline{C}_{12}]$$

$$\overline{G}_2 = \frac{[\overline{S}_{11}\overline{S}_{22} - \overline{S}_{12}\overline{S}_{21}][\overline{C}_{11} + \overline{C}_{22}]}{[\overline{S}_{11}\,\overline{C}_{22} + \overline{S}_{22}\overline{C}_{11} - \overline{S}_{12}\,\overline{C}_{21} - \overline{S}_{21}\,\overline{C}_{12}]} \tag{3.33}$$

$$\overline{G}_3 = \frac{[\overline{S}_{11}\overline{C}_{11} + \overline{S}_{12}\,\overline{C}_{12} + \overline{S}_{21}\,\overline{C}_{21} + \overline{S}_{22}\,\overline{C}_{22}\,]}{[\overline{C}_{11} + \overline{C}_{12}\,]}$$

The performance characteristics of non-recessed hole-entry hybrid journal bearing system are computed by solving the governing system equations described earlier.

3.9 SOLUTION PROCEDURE

This chapter presents the overall solution scheme to obtain the solution of the constant flow valve compensated non-recessed hole-entry hybrid journal bearing system. The analysis of the compensated hybrid journal bearing requires the simultaneous solution of modified Reynolds equation (3.9) together with equation of flow of the lubricant through the restrictor as a constraint. This requires an iterative technique to obtain the matched solutions. Additional iterations are also required for the establishment of equilibrium journal centre position for a specified vertical load. When journal center equilibrium is attained then the static and dynamic performance characteristics of the journal bearing system are computed.

Fig. 3.2 shows the over all solution schemes employed for the solution of compensated hole-entry hybrid journal bearing system. The over all solution consists of following stages.

- Initially, the unit LDAT reads the input data and 2-D lubrication mesh.
- Then the unit FLM calculates the values of fluid film thickness at nodal points given by equation (3.29) utilizing tentative values of $\overline{X}_J$ and $\overline{Z}_J$.

- Then the unit TRBU calculates the values of turbulent coefficients (G_α andG_β) given by equations (3.7) and (3.8).
- Using the nodal values of fluid film thickness, the element fluidity matrices of equation (3.17) are generated and assembled in the unit FLD.
- Then the unit BDRY modifies the system equation for specified boundary conditions.
- The modified system equations are then solved for the values of nodal pressure in unit SVG using Gaussian elimination technique.
- The pressure field for the lubrication flow field obtained, from BLOCK PRS as shown in Fig. 3.2.
- Then the unit STATCH & DYNACH calculates the static and dynamic characteristics of journal bearing system.
- Then the unit LPRINT prints the calculated data and then unit STOP terminates the program.

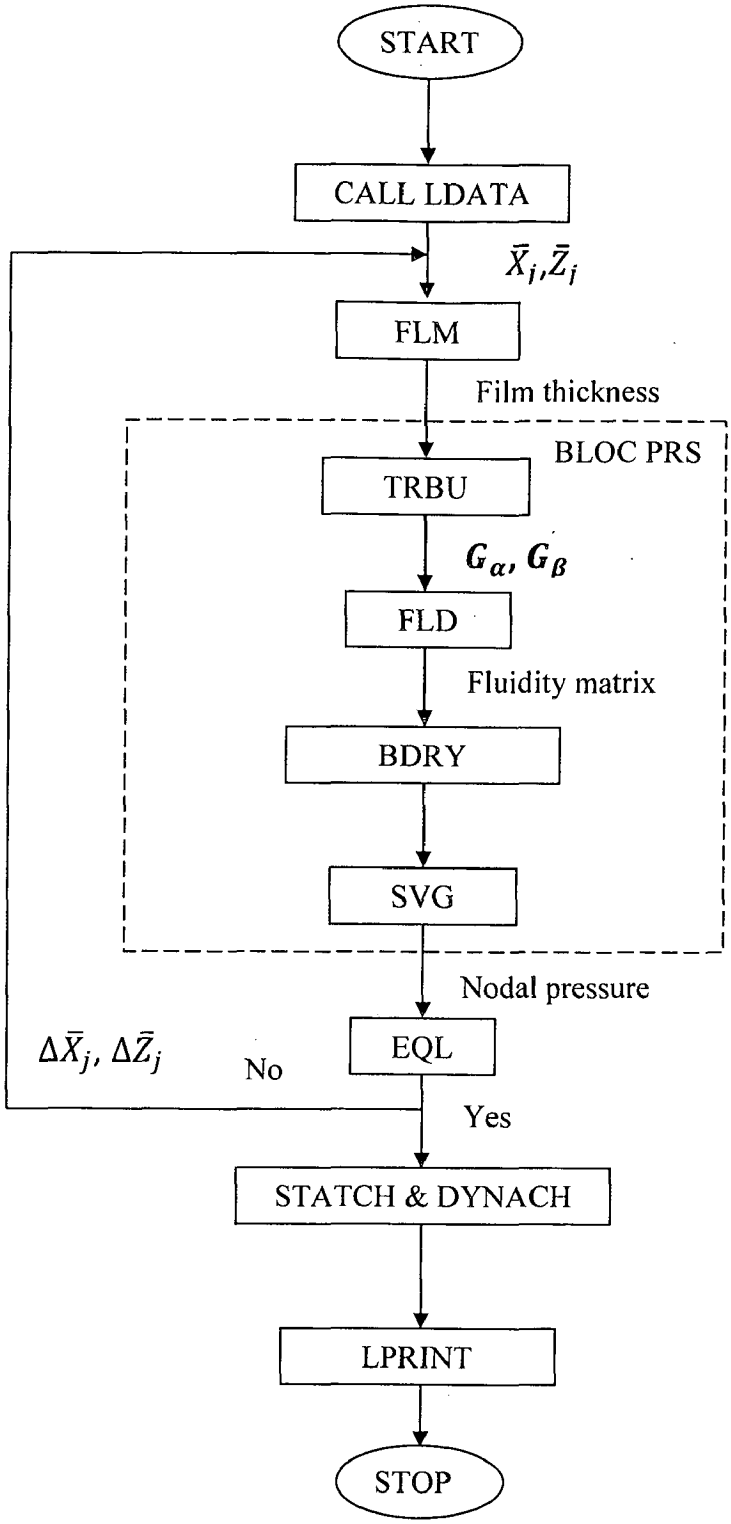

Fig. 3.2 Overall solution scheme to obtain the solution of the compensated hybrid journal bearing

CHAPTER- 4 RESULTS & DISCUSSION

The analysis and solution algorithm presented in the previous chapters were used to compute the performance characteristics of non-recessed hole-entry hybrid journal bearing system operating in turbulent regime. The static and dynamic performance characteristics which include maximum pressure ($\overline{p}_{max}$), minimum film thickness ($\overline{h}_{min}$), bearing flow ($\overline{Q}$), frictional torque ($\overline{T}_{fric}$), stiffness coefficients ($\overline{S}_{11}, \overline{S}_{22}$), damping coefficients ($\overline{C}_{11}, \overline{C}_{22}$) and stability threshold speed margin ($\overline{\omega}_{th}$) have been presented for the non-recessed hole-entry hybrid journal bearing configurations. The results have been presented for two separate cases. The numerically simulated results have been presented through Fig. 4.2 to Fig. 4.35 for the chosen bearing operating and geometric parameters as shown in table 4.1.

1. **Influence of turbulence on the performance of unworn hole-entry hybrid journal bearing system.**

The computed results have been presented through Fig. 4.2 to Fig. 4.17 for a constant flow valve compensated non-recessed hole-entry Symmetric/asymmetric hybrid journal bearing configurations operates in turbulent regime.

(i) Variation of performance characteristic parameters with external load ($\overline{W}_o$) for different values of Reynolds number.

(ii) Variation of performance characteristic parameters with restrictor design parameter ($\overline{C}_{s2}$) for different values of Reynolds number.

2. **Influence of turbulence on the performance of worn hole-entry hybrid journal bearing system.**

The computed results have been presented through Fig. 4.18 to Fig. 4.35 for worn hole-entry hybrid journal bearing compensated with different restrictors operating in turbulent regime.

(iii) Variation of performance characteristic parameters with wear depth parameter ($\bar{\delta}_w$) for different values of Reynolds number.

(iv) Variation of performance characteristic parameters with Reynolds number (R_e) for different values of wear depth parameter ($\bar{\delta}_w$).

4.1 VALIDATION

Based on the analysis and the solution algorithms presented in chapter-3, a computer program has been developed to analyze the performance characteristics of non-recessed hole-entry hybrid journal bearing compensated with constant flow valve restrictor considering the influence of turbulence. The performance of a worn hybrid journal bearing system operating in turbulent regime has also been studied. To the best knowledge of the author, no published data is yet available on the performance of constant flow valve compensated non-recessed hole-entry hybrid journal bearing operating in turbulent regime. Therefore, In order to validate the methodology of the developed program, the computed results have been compared with already available results of hydrodynamic journal bearing operating in turbulent regime [39]. The present results are compared with already published results of Kumar and Mishra [39] as shown in Fig. 4.1 and it has been found that the results are in good agreement.

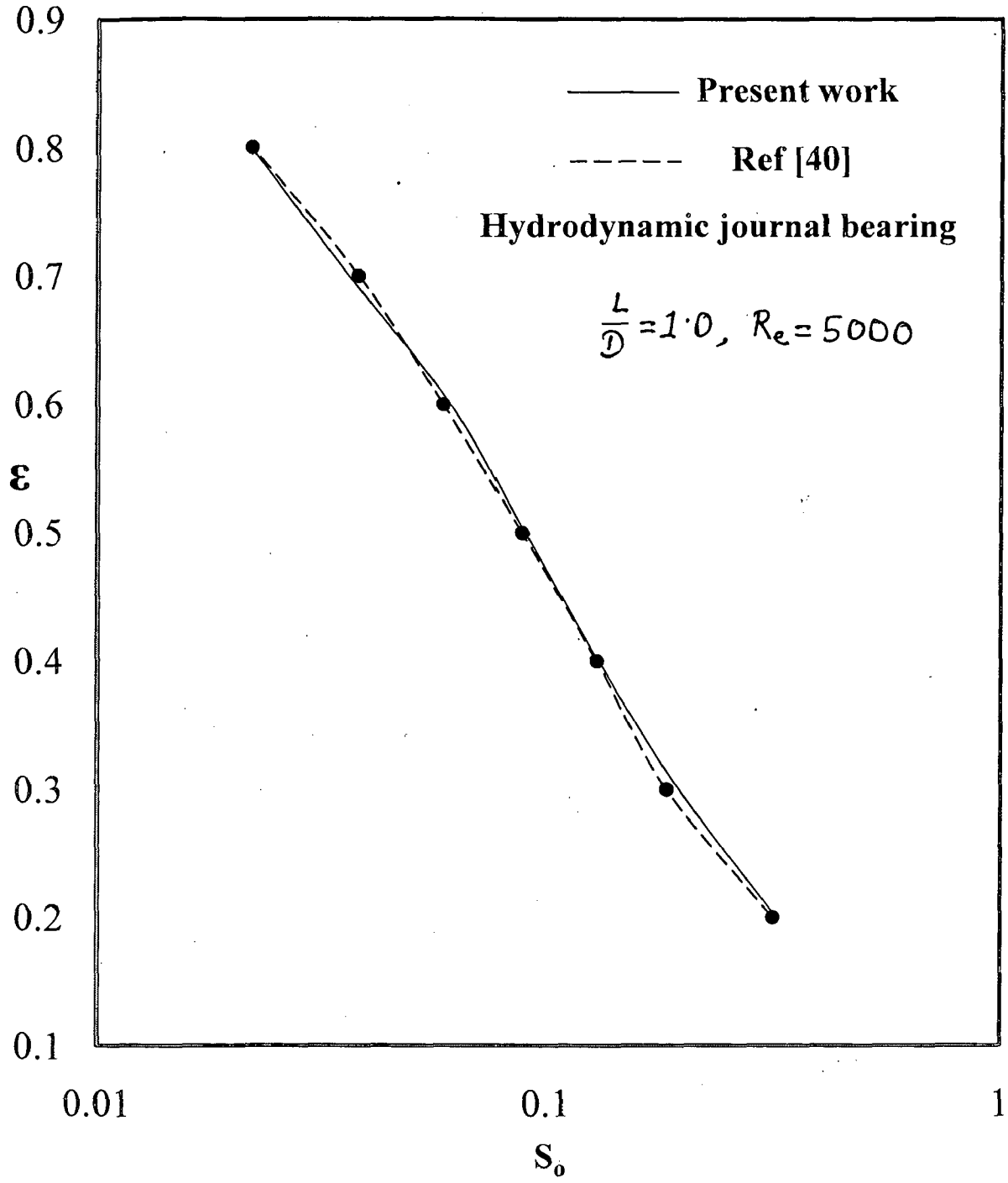

Fig. 4.1 Variation of eccentricity (ε) with Sommerfeld number (S_o)

4.2 RESULTS & DISCUSSION

1. Influence of turbulence on the performance of unworn hole-entry hybrid journal bearing system.

Fig. 4.2 shows the variation of maximum fluid film pressure ($\bar{p}_{max}$) for both symmetric and asymmetric configurations of hole-entry hybrid journal bearing with external load ($\bar{W}_o$). It has been observed that the increasing trend for the value of $\bar{p}_{max}$ is found in case of symmetric configuration where as for asymmetric configuration reversed trend is observed when bearing operates in turbulent regime. It may be observed that the value of $\bar{p}_{max}$ increases by 62.95% for external load range $\bar{W}_o = 0.25 - 1.5$ when symmetric journal bearing operates in laminar regime. However, as the value of turbulence increases the value of $\bar{p}_{max}$ increases significantly at any constant value of external load $\bar{W}_o$ as compared to bearing operates in laminar regime. In case of asymmetric configuration of hole-entry hybrid journal bearing, as the value of Reynolds number increases, the percentage increase in the value of $\bar{p}_{max}$ is found to be order of 84.57% for the value of $R_e = 20000$ at external load $\bar{W}_o = 1.5$ as compared to symmetric journal bearing operates in laminar regime.

Fig. 4.3 depicts the variation of minimum fluid film thickness ($\bar{h}_{min}$) for symmetric as well as asymmetric configurations. The decreasing trend for the value of minimum fluid film thickness has been observed for symmetric configuration of bearing, but in case of asymmetric configuration a reversed trend is found when bearing operates in turbulent regime. It is also observed that the value of $\bar{h}_{min}$ first increases for load range $\bar{W}_o = 0.25 - 0.75$ and then decreases when asymmetric bearing operates in laminar regime. It may be observed that the value of $\bar{h}_{min}$ decreases by 12.91% for external load range $\bar{W}_o = 0.25 - 1.5$ when symmetric journal bearing operates in laminar regime. In case of symmetric configuration of hole-entry hybrid journal bearing due to effect of turbulence for the value of $R_e = 20000$, the loss in the value of $\bar{h}_{min}$ gets compensated by 13.57% at external load $\bar{W}_o = 1.5$ as compared to symmetric journal bearing operates in laminar regime where as for asymmetric journal bearing the value of $\bar{h}_{min}$ is increased by 12.05% for same value of R_e and $\bar{W}_o$ compared to symmetric journal bearing operates in laminar regime.

From the Fig. 4.4 similar trend of frictional torque ($\bar{T}_{fric}$) has been observed for symmetric as well as asymmetric configurations as a function of external load ($\bar{W}_o$). Due to influence of turbulence, the value of $\bar{T}_{fric}$ get increased significantly for higher value of Reynolds number for symmetric as well as asymmetric configuration, but in asymmetric configuration of bearing the value of $\bar{T}_{fric}$ is found to be marginally higher at constant value of external load, $\bar{W}_o = 0.5$ for higher value of R_e when bearing operates in laminar as well as turbulent regime.

Fig. 4.5 & Fig. 4.6 show the variation for the value of direct fluid film stiffness coefficients ($\bar{S}_{11}, \bar{S}_{22}$). It has been observed that the value of $\bar{S}_{11}$ & $\bar{S}_{22}$ is higher for symmetric configuration as compared to asymmetric configuration of bearing at constant value of $\bar{W}_o$ when the bearing operates in both laminar and turbulent regime. In case of symmetric configuration of bearing due to effect of turbulence for the higher value of R_e, the values of $\bar{S}_{11}$ & $\bar{S}_{22}$ gets increased significantly at constant value of $\bar{W}_o$ as compared to symmetric bearing operates in laminar regime where as for asymmetric configuration of bearing, the values of $\bar{S}_{11}$ & $\bar{S}_{22}$ is found to be order of 39.16% and 149.66% for same value of $R_e = 20000$ at $\bar{W}_o = 1.5$ as compared to symmetric bearing operates in laminar regime at $\bar{W}_o = 1.5$.

Fig. 4.7 & Fig. 4.8 show the same trend for the values of direct fluid film damping coefficients ($\bar{C}_{11}, \bar{C}_{22}$) for symmetric as well as asymmetric configurations of bearing with $\bar{W}_o$. It has been observed that the value of $\bar{C}_{11}$and $\bar{C}_{22}$ is marginally higher for asymmetric configuration as compared to symmetric configuration of bearing at any constant value of $\bar{W}_o$ when the bearing is operating at higher values of R_e. It may be observed that the value of $\bar{C}_{11}$and $\bar{C}_{22}$ increases, as the value of R_e increases for both symmetric/asymmetric configurations of bearing at constant value of $\bar{W}_o$.

Fig. 4.9 depicts the variation of threshold speed margin ($\bar{\omega}_{th}$) for symmetric as well as asymmetric configurations with $\bar{W}_o$. It has been observed that the value of $\bar{\omega}_{th}$ gets decreases with an increase in the value of $\bar{W}_o$ for both symmetric as well as asymmetric configurations when bearing operates in both laminar and turbulent regimes. It may be noted that the value of $\bar{\omega}_{th}$ is more for symmetric configuration as compared to asymmetric configuration at constant value of external load. Further, it has been observed that the value of $\bar{\omega}_{th}$ decreased by 57.30%

for external load range $\bar{W}_o = 0.25 - 1.5$ when symmetric bearing operates in laminar regime. However, for the value of $R_e = 20000$, the loss in the value of $\bar{\omega}_{th}$ gets compensated by 97.02% at $\bar{W}_o = 1.5$ as compared to symmetric bearing operates in laminar regime where as in case of asymmetric bearing the value of $\bar{\omega}_{th}$ gets compensated by 38.72% for same value of R_e and $\bar{W}_o$ compared to symmetric bearing operates in laminar regime.

Fig. 4.10 shows variation for the value of maximum fluid film pressure ($\bar{p}_{max}$) for symmetric and asymmetric configurations of bearing with $\bar{C}_{s2}$. It has been observed that the value of $\bar{p}_{max}$ increases for symmetric as well as asymmetric configurations of bearing when bearing is operating in laminar as well as turbulent regime. It has been observed for symmetric as well as asymmetric configurations of journal bearing, due to influence of turbulence the value of $\bar{p}_{max}$ gets increased significantly for large value of Reynolds number as compared to symmetric bearing operates in laminar regime at $\bar{C}_{s2} = 0.25$.

Fig. 4.11 depicts the variation of minimum fluid film thickness ($\bar{h}_{min}$) as a function of $\bar{C}_{s2}$. It has been noted that the increasing trend for the value of $\bar{h}_{min}$ is observed for symmetric configuration where as in case of asymmetric configuration a reversed trend is observed when bearing operates in both laminar and turbulent regime. For the constant value of $\bar{C}_{s2} = 0.25$ symmetric configuration of bearing, the value of $\bar{h}_{min}$ found to be higher than that of asymmetric configuration. Further, the increase in the value of $\bar{h}_{min}$ found to be order of 9.25% for the range of $\bar{C}_{s2} = 0.05 - 0.25$ when symmetric bearing operates in laminar regime. However, due to influence of turbulence, for the higher value of $R_e = 20000$ the value of $\bar{h}_{min}$ gets increased by 3.22% for symmetric configuration of journal bearing compared to symmetric journal bearing operates in laminar regime at $\bar{C}_{s2} = 0.25$ where as in case of asymmetric configuration due non symmetric presence of holes the value of $\bar{h}_{min}$ gets decreased by 19.47% and 20.62% for $R_e = 10000$ and 20000 respectively compared to symmetric journal bearing operates in laminar regime at $\bar{C}_{s2} = 0.25$.

Fig. 4.12 shows the variation for the value of frictional torque ($\bar{T}_{fric}$) for symmetric and asymmetric configurations of bearing with $\bar{C}_{s2}$. It may be observed that the value of $\bar{T}_{fric}$ increases for higher values of R_e for symmetric and asymmetric configurations, when bearing

operates in turbulent regime. Further it has also been noted that the value of $\bar{T}_{fric}$ is marginally higher for asymmetric configuration than that of symmetric configuration of bearing.

Fig. 4.13 and Fig. 4.14 depicts the variation for the values of direct fluid film stiffness coefficients ($\bar{S}_{11}, \bar{S}_{22}$) for symmetric as well as asymmetric configurations of bearing with $\bar{C}_{s2}$. The increasing trend has been observed for the values of $\bar{S}_{11}$ & $\bar{S}_{22}$ for symmetric and asymmetric configurations, for the range of $\bar{C}_{s2} = 0.05 - 0.25$ when bearing operates in both laminar as well as turbulent regime. It has been observed that for constant value of $\bar{C}_{s2}$, the value of direct fluid film stiffness coefficients ($\bar{S}_{11}, \bar{S}_{22}$) is found to be higher for case of symmetric configuration than that of asymmetric configuration of bearing when bearing operates in turbulent regime. The percentage of increase in the value of $\bar{S}_{11}$ and $\bar{S}_{22}$ is found to be order of 321.97% and 319.99% for the value of $R_e = 20000$ respectively for symmetric configuration as compared to symmetric bearing operates in laminar regime at $\bar{C}_{s2} = 0.25$ where as in case of asymmetric configuration the percentage of increase in the value of $\bar{S}_{11}$ and $\bar{S}_{22}$ is found to be order of 20.19% and 167.65% for the same value of R_e at constant value of $\bar{C}_{s2}$ as compared to symmetric bearing operates in laminar regime.

The similar trend has been observed from Fig. 4.15 and Fig. 4.16 for the values of direct fluid film damping coefficients ($\bar{C}_{11}, \bar{C}_{22}$) with restrictor design parameter. It may be noted that the value of $\bar{C}_{11}$ & $\bar{C}_{22}$ is higher for asymmetric configuration of bearing than that of symmetric configuration at constant value of $\bar{C}_{s2}$ when bearing operates in both laminar as well as turbulent regime. it may also be noted that, for the value of $R_e = 20000$, the percentage of increase in the value of $\bar{C}_{11}$ and $\bar{C}_{22}$ is found to be order of 324.52% and 323.07% respectively for symmetric configuration as compared to symmetric bearing operates in laminar regime at $\bar{C}_{s2} = 0.25$ where as in case of asymmetric configuration the percentage of increase in the value of $\bar{C}_{11}$ and $\bar{C}_{22}$ is found to be order of 393.55% and 384.02% for the same value of R_e and $\bar{C}_{s2}$ as compared to symmetric bearing operates in laminar regime.

Fig. 4.17 shows the variation of stability threshold speed margin $\bar{\omega}_{th}$. The increasing trend has been observed for the value of $\bar{\omega}_{th}$ for symmetric and asymmetric configurations of bearing when bearing operates in both laminar as well as turbulent regime. Further, it has been observed that the value of $\bar{\omega}_{th}$ increases by 117.75% for the range of $\bar{C}_{s2} = 0.05 - 0.25$ when

symmetric bearing operates in laminar regime. However, the percentage increases in the value of $\bar{\omega}_{th}$ for the value of $R_e = 5000, 10000$ and 20000 is found to be order of 47.16%, 71.20% and 105.02% respectively for symmetric configuration of journal bearing at $\bar{C}_{s2} = 0.25$ compared to symmetric bearing operates in laminar regime where as in case of asymmetric configuration, the percentage of increase in the value of $\bar{\omega}_{th}$ for the same value of Reynolds number is found to be order of 18.01%, 40.18% and 71.25% respectively at $\bar{C}_{s2} = 0.25$ as compared to symmetric bearing operates in laminar regime at $\bar{C}_{s2} = 0.25$.

2. **Influence of turbulence on the performance of worn hole-entry hybrid journal bearing system.**

The variation of minimum fluid film thickness ($\bar{h}_{min}$) with wear depth parameter ($\bar{\delta}_w$) is shown in Fig. 4.18 for different values of Reynolds number (R_e). It may be observed that the value of $\bar{h}_{min}$ decreases with an increase in the wear depth parameter $\bar{\delta}_w$ for constant flow valve, orifice and capillary compensated bearings operates in both laminar/turbulent regimes. It may be observed that the value of $\bar{h}_{min}$ is more for constant flow valve compensated bearing as compared to both capillary and orifice compensated bearings at constant value of $\bar{\delta}_w$. The percentage decrease in the value of $\bar{h}_{min}$ is found to be order of 14.17% for constant flow valve compensated bearing operates in laminar regime for the range of $\bar{\delta}_w = 0.0 - 0.5$. However, for the constant value of $R_e = 10000$ the percentage of increase in the value of $\bar{h}_{min}$ for constant flow valve compensated bearing is 17.59% and the reduction in the value of $\bar{h}_{min}$ for capillary and orifice compensated bearing is found to be order of 11.30% and 2.06% respectively at $\bar{\delta}_w = 0.5$ as compared to constant flow valve compensated bearing operates in laminar regime.

Fig. 4.19 depicts the variation of frictional torque ($\bar{T}_{fric}$) with wear depth parameter ($\bar{\delta}_w$). It may be noted that the value of $\bar{T}_{fric}$ is lower for constant flow valve compensated bearing as compared to both capillary and orifice compensated bearings at constant value of $\bar{\delta}_w$ when bearing operates in laminar as well as turbulent regimes. The percentage of reduction in the value of $\bar{T}_{fric}$ is found to be order of 5.21% for constant flow valve compensated bearing operates in laminar regime for the range of $\bar{\delta}_w = 0 - 0.5$. Further for the value of $R_e = 10000$, the value of $\bar{T}_{fric}$ increases significantly for constant flow valve, capillary and orifice compensated bearings

at constant value of $\bar{\delta}_w = 0.5$ as compared to constant flow valve compensated bearing operates in laminar regime.

Fig. 4.20 and Fig. 4.21 show the same trend for the value of direct fluid film stiffness $(\bar{S}_{11}, \bar{S}_{22})$ with wear depth parameter $(\bar{\delta}_w)$. It may be noted that the value of $\bar{S}_{11}$ and $\bar{S}_{22}$ is more for constant flow valve compensated bearing as compared to both capillary and orifice compensated bearings at constant values of $\bar{\delta}_w$. Further, it has been observed that the percentage decrease in the value of $\bar{S}_{11}$ and $\bar{S}_{22}$ is found to be order of 22.76% and 30.77% for constant flow valve compensated bearing operates in laminar regime for the range of $\bar{\delta}_w = 0 - 0.5$. However, at the value of $R_e = 10000$ the percentage increase in the value of $(\bar{S}_{11}, \bar{S}_{22})$ for constant flow valve compensated bearing is (192.58%, 128.96%) and the percentage reduction in the value of $(\bar{S}_{11}, \bar{S}_{22})$ for capillary and orifice compensated bearings (45.46%, 36.42%) and (38.31%, 18.68%) respectively at constant value of $\bar{\delta}_w = 0.5$ as compared to constant flow valve compensated bearing operates in laminar regime.

Fig. 4.22 and Fig. 4.23 depict the variation for the value of direct fluid film damping coefficients $(\bar{C}_{11}, \bar{C}_{22})$ with $\bar{\delta}_w$. It may be noted that the value of $\bar{C}_{11}$ and $\bar{C}_{22}$ is higher for constant flow valve compensated bearing as compared to both capillary and orifice compensated bearings at constant value of $\bar{\delta}_w$ when bearing operates in turbulent regime. Further, it has been observed that the percentage of reduction in the value of $\bar{C}_{11}$ and $\bar{C}_{22}$ is found to be order of 16.77% and 26.76% for constant flow valve compensated bearing operates in laminar regime for the range of $\bar{\delta}_w = 0 - 0.5$. However, for the higher value of R_e the percentage increase in the value of $(\bar{C}_{11}, \bar{C}_{22})$ is found to be order of (197.14%, 150.42%), (30.69%, 20.26%) and (34.18%, 16.46%) for constant flow valve, capillary and orifice compensated bearings respectively at constant value of $\bar{\delta}_w = 0.5$ as compared to constant flow valve compensated bearing operates in laminar regime.

Fig. 4.24 shows variation of threshold speed margin $(\bar{\omega}_{th})$ as a function of wear depth parameter $(\bar{\delta}_w)$. It may be observed that the value of $\bar{\omega}_{th}$ is more for constant flow valve compensated bearing as compared to both capillary and orifice compensated bearings at constant value of $\bar{\delta}_w$ when bearing is operating in both laminar/turbulent regimes. The percentage of reduction in the value of $\bar{\omega}_{th}$ is found to be order of 9.22% for constant flow valve compensated

bearing operates in laminar regime for the range of $\bar{\delta}_w = 0.0 - 0.5$. Further, it has been noted for the value of $R_e = 10000$, the percentage of increase in the value of $\bar{\omega}_{th}$ is found to be order of 59.44%, for constant flow valve compensated bearing where as in case of capillary and orifice compensated bearings the percentage of reduction in the value of $\bar{\omega}_{th}$ is found of the order of 28.03% and 21.42% respectively at constant value of $\bar{\delta}_w = 0.5$ as compared to constant flow valve compensated bearing operates in laminar regime.

Fig. 4.25 shows increasing trend for the value of minimum fluid film thickness ($\bar{h}_{min}$) with Reynolds number (R_e). It may be observed that the value of $\bar{h}_{min}$ is more for constant flow valve compensated bearing as compared to both capillary and orifice compensated bearings at the constant value of R_e for different values of $\bar{\delta}_w$. Further, at $\bar{\delta}_w = 0.5$, the percentage of increase in the value of $\bar{h}_{min}$ is found to be order of 13.70% for the range of $R_e = 0 - 10000$, for constant flow valve compensated bearing operates in laminar regime. Further, it may be noted that the due to influence of turbulence, the value of $\bar{h}_{min}$ decreases for constant flow valve, capillary and orifice compensated bearings operates in laminar as well as turbulent regime. For the constant value of $\bar{\delta}_w = 0.5$ the percentage decrease in the value of $\bar{h}_{min}$ is found to be order of 11.24%, 33.05% and 26.07% for constant flow valve, capillary and orifice compensated bearings respectively at the value of $R_e = 10000$ as compared to constant flow valve compensated bearing operates in laminar regime.

Fig. 4.26 shows variation for the value of frictional torque ($\bar{T}_{fric}$) with Reynolds number (R_e) for different values of $\bar{\delta}_w$. It has been observed that the value of $\bar{T}_{fric}$ increases as the Reynolds number increases when bearing operates in laminar as well as turbulent regimes. It is interesting to notice that the frictional torque decreases with increase in the value of $\bar{\delta}_w$ at constant value of R_e. Further, at the value of $\bar{\delta}_w = 0.5$ the percentage of reduction in the value of $\bar{T}_{fric}$ is found to be order of 7.49%, 4.14% and 5.75% for constant flow valve, capillary and orifice compensated bearings respectively at constant value of $R_e = 10000$ as compared to constant flow valve compensated bearing operates in laminar regime.

Fig. 4.27 and Fig. 4.28 show the same trend for the variation of direct fluid film stiffness ($\bar{S}_{11}, \bar{S}_{22}$). It may be noted that the value of $\bar{S}_{11}$ and $\bar{S}_{22}$ is more for constant flow valve compensated bearing as compared to both capillary and orifice compensated bearings for

different values of $\bar{\delta}_w$ at constant value of R_e. Further, it has been observed that the percentage increase in the value of $\bar{S}_{11}$ and $\bar{S}_{22}$ is found to be order of 181.11% and 162.41% for constant flow valve compensated bearing operates in laminar regime for the range of $R_e = 0 - 10000$. However, it is interesting to notice that the value of wear depth parameter increases the value of $\bar{S}_{11}$ and $\bar{S}_{22}$ gets reduced at constant value of R_e when bearing operates in turbulent regime. Further, it has been observed at the constant value of $\bar{\delta}_w = 0.5$ the percentage of reduction in the value of $(\bar{S}_{11}, \bar{S}_{22})$ is found to be order of (19.60%, 39.59%), (85.01%, 83.22%) and (83.05%, 78.54%) for constant flow valve, capillary and orifice compensated bearings for the value of $R_e = 10000$ as compared to constant flow valve compensated bearing operates in laminar regime.

Fig. 4.29 and Fig. 4.30 show the variation of direct fluid film damping coefficients $(\bar{C}_{11}, \bar{C}_{22})$ with Reynolds number (R_e). It may be noted that the value of $\bar{C}_{11}$ and $\bar{C}_{22}$ is larger for constant flow valve compensated bearing compared to both capillary and orifice compensated bearings for different values of $\bar{\delta}_w$ at any constant value of R_e. Further, it has been observed that the percentage increase in the value of $\bar{C}_{11}$ and $\bar{C}_{22}$ is found to be order of 187.54% and 174.31% for constant flow valve compensated bearing operates in laminar regime when for the range of $R_e = 0 - 10000$. However, it is interesting to notice that as the wear depth increases, the value of $\bar{C}_{11}$ and $\bar{C}_{22}$ gets reduced at constant value of R_e when bearing operates in turbulent regime. For the constant value of $\bar{\delta}_w = 0.5$ the percentage of reduction in the value of $(\bar{C}_{11}, \bar{C}_{22})$ is found to be order of (13.99%,33.14%), (62.17%,67.89%) and (61.16%,65.96%) for constant flow valve, capillary and orifice compensated bearings respectively at constant value of $R_e = 10000$ as compared to constant flow valve compensated bearing operates in laminar regime.

Fig. 4.31 shows the variation for the value of stability threshold speed margin $(\bar{\omega}_{th})$. It may be observed that the value of $\bar{\omega}_{th}$ is larger for constant flow valve compensated bearing compared to both capillary and orifice compensated bearings for different values of $\bar{\delta}_w$ at constant value of R_e when bearing operates in laminar as well as turbulent regime. Further, for constant value of $\bar{\delta}_w = 0.5$ the percentage increase in the value of $\bar{\omega}_{th}$ is found to be order of 61.68% for constant flow valve compensated bearing operates with the range of $R_e = 0 - 10000$. It is interesting to notice that the value of $\bar{\omega}_{th}$ decreases with increase in the value of $\bar{\delta}_w$ at constant value of R_e for all bearing configurations studied. Further it may be noted that at the

constant value of $\bar{\delta}_w = 0.5$ the decrease in the value of $\bar{\omega}_{th}$ is found to be order of 10.47%, 59.59% and 55.88% for constant flow valve, capillary and orifice compensated bearings respectively at constant value of $R_e = 10000$ as compared to constant flow valve compensated bearing operates in laminar regime.

CHAPTER- 5 CONCLUSIONS

5.1 CONCLUSIONS

The work reported in the thesis presents a theoretical study concerning the influence of turbulence on performance characteristics parameters of a non-recessed hole-entry hybrid journal bearing system for both symmetric as well as asymmetric configurations. The study of wear due to start/stop operations has also been carried on the constant floe valve, capillary and orifice compensated hole-entry hybrid journal bearing system. On the basis of analysis, solution algorithm and results presented in previous chapters by considering the effect of wear and turbulence, the following conclusions are drawn for the given values of bearing geometric and operating parameters.

5.1.1 Influence of turbulence on performance characteristics parameters:-

- The bearing performance characteristics parameters get affected appreciably due to influence of turbulence on hole-entry hybrid journal bearing system.
- It may be observed that the value of $\bar{h}_{min}$ gets compensated by 13.57% for $R_e = 20000$ at $\bar{W}_o = 1.5$ as compared to the bearing operates in laminar regime at $\bar{W}_o = 1.5$ where as in asymmetric bearing configuration a reversed trend for the value of $\bar{h}_{min}$ has been observed. Further, the value of $\bar{h}_{min}$ gets increased by 3.22% for $R_e = 20000$ at $\bar{C}_{s2} = 0.25$ for symmetric bearing configuration where as in case of asymmetric bearing configuration the value of $\bar{h}_{min}$ gets reduced by 20.62% for $R_e = 20000$ at $\bar{C}_{s2} = 0.25$ as compared to symmetric bearing operates in laminar regime.
- The frictional torque ($\bar{T}_{fric}$) increases for both symmetric as well as asymmetric bearing configurations when operating in turbulent regime.
- The direct fluid film stiffness coefficients ($\bar{S}_{11}, \bar{S}_{22}$) increases significantly for symmetric bearing configuration than that of asymmetric bearing configuration when bearing operating in turbulent regime.
- It is observed that the direct fluid film damping coefficients ($\bar{C}_{11}, \bar{C}_{22}$) are more for asymmetric bearing configuration than that of symmetric bearing configuration for the higher values of Reynolds number $R_e = 20000$.

- The stability threshold speed margin ($\bar{\omega}_{th}$) is higher for symmetric bearing configuration than that of asymmetric bearing configuration when bearing operates in turbulent regime. The percentage of increase in the value of $\bar{\omega}_{th}$ is found to be order of 97.02% and 38.72% for both symmetric and asymmetric bearing configurations for the Reynolds number $R_e = 20000$ at $\bar{W}_o = 1.5$ respectively as compared to symmetric bearing operates in laminar regime. Further, it has been observed that the percentage of increase in the value of $\bar{\omega}_{th}$ for $R_e = 5000, 10000$ and 20000 is found to be order of 47.16%, 71.20% and 105.02% respectively for symmetric bearing configuration where as in case of asymmetric bearing configuration the percentage of increase in the value of $\bar{\omega}_{th}$ for the same value of R_e is found to be order of 18.01%, 40.18% and 71.25% respectively at $\bar{C}_{s2} = 0.25$ as compared to symmetric bearing operates in laminar regime.

5.1.2 Combined influence of wear and turbulence on performance characteristics parameters:-

- It has been observed that the value of $\bar{h}_{min}$ gets reduced as the value of wear depth parameter increases. However, due to combined influence of wear and turbulence the value of $\bar{h}_{min}$ gets increased for the value of $R_e = 10000$ and the maximum percentage of increase in the value of $\bar{h}_{min}$ is found to be order of 17.59% for constant flow valve compensated bearing at $\bar{\delta}_w = 0.5$ as compared to constant flow valve compensated bearing operates in laminar regime.
- The frictional torque ($\bar{T}_{fric}$) for constant flow valve compensated bearing is lower due to the combined influence of wear and turbulence as compared to capillary and orifice compensated bearings operating in both laminar as well as turbulent regimes.
- It has been observed that due to combined influence of wear and turbulence, the direct fluid film stiffness and damping coefficients $((\bar{S}_{11}, \bar{S}_{22})\ \&\ (\bar{C}_{11}, \bar{C}_{22}))$ gets increased significantly with the higher values of Reynolds number for constant flow valve compensated bearing as compared to capillary and orifice compensated bearings operating in both laminar as well as turbulent regimes.
- The percentage of increase in the value of $\bar{\omega}_{th}$ is found to be order of 59.44% for constant flow valve compensated bearing due to combined influence of wear and turbulence where as for capillary and orifice compensated bearings, the value of $\bar{\omega}_{th}$ is reduced by 28.03%

and 21.42% respectively at constant wear depth parameter $\bar{\delta}_w = 0.5$ as compared to constant flow valve compensated bearing operates in laminar regime.

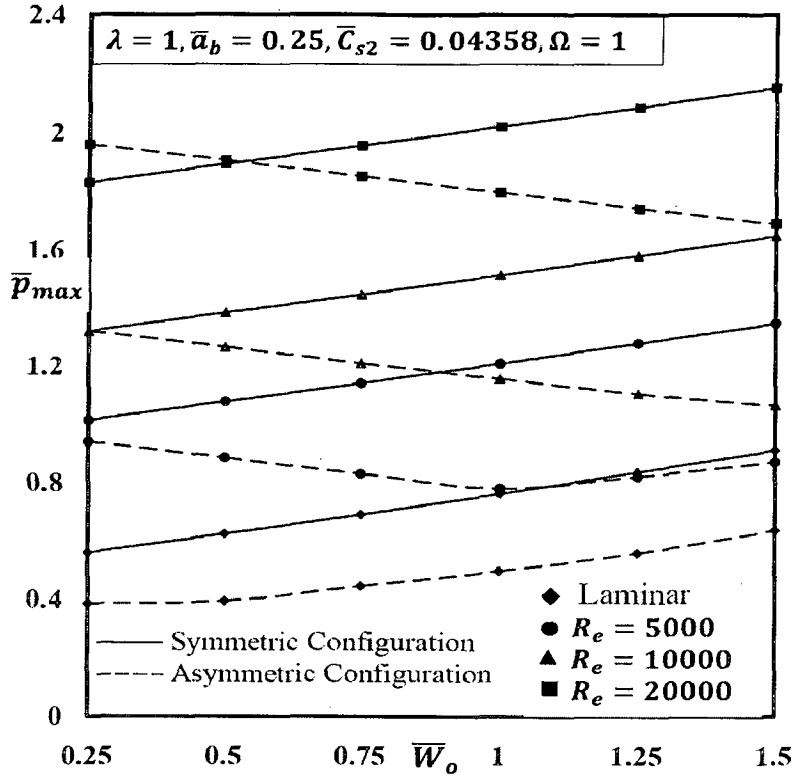

Fig. 4.2 Variation of with

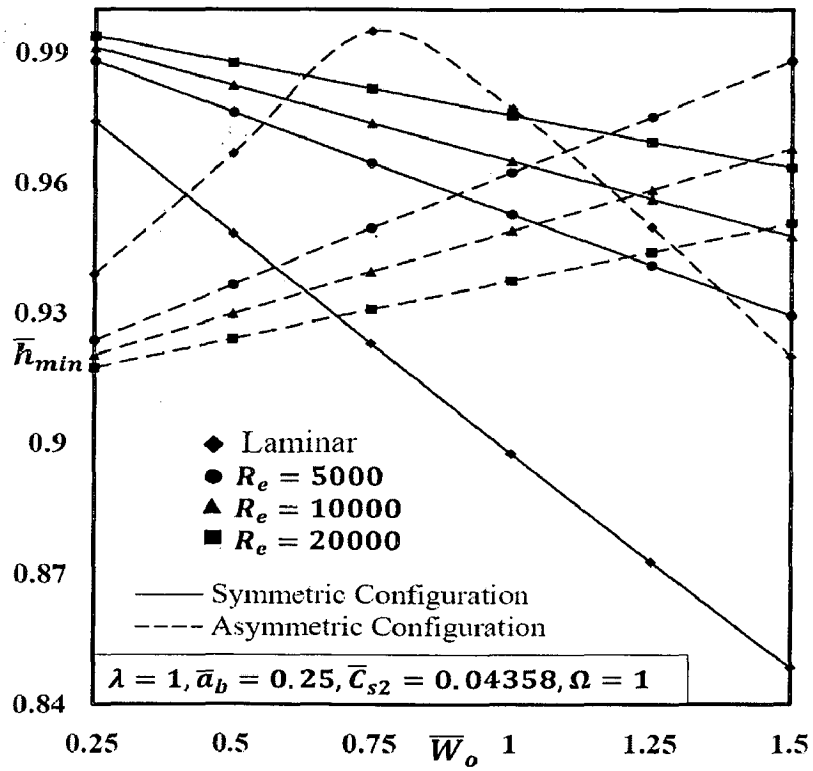

Fig. 4.3 Variation of with

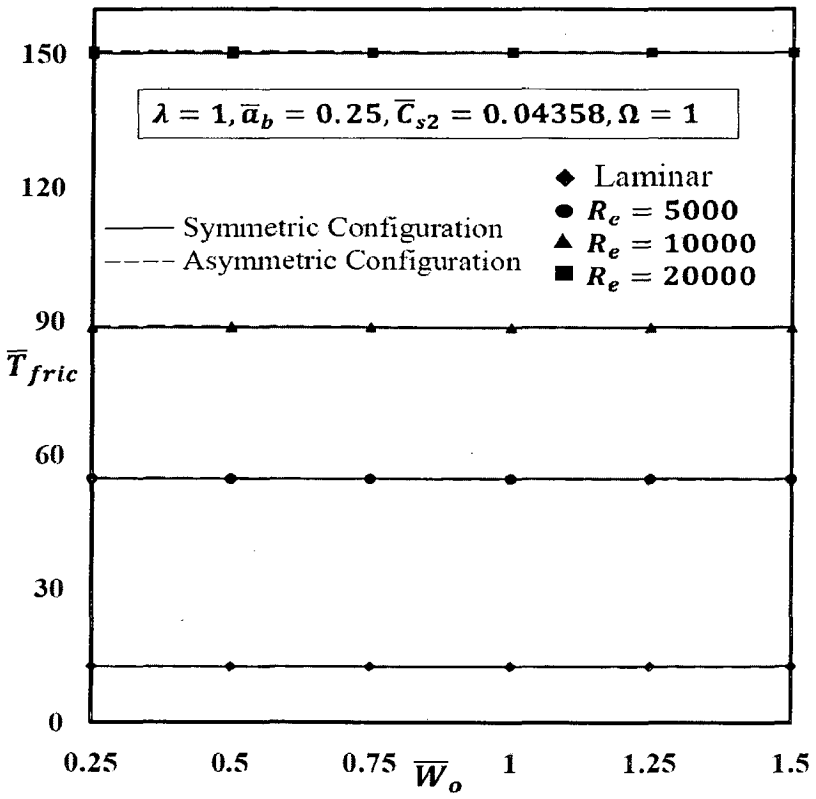

Fig. 4.4 Variation of with

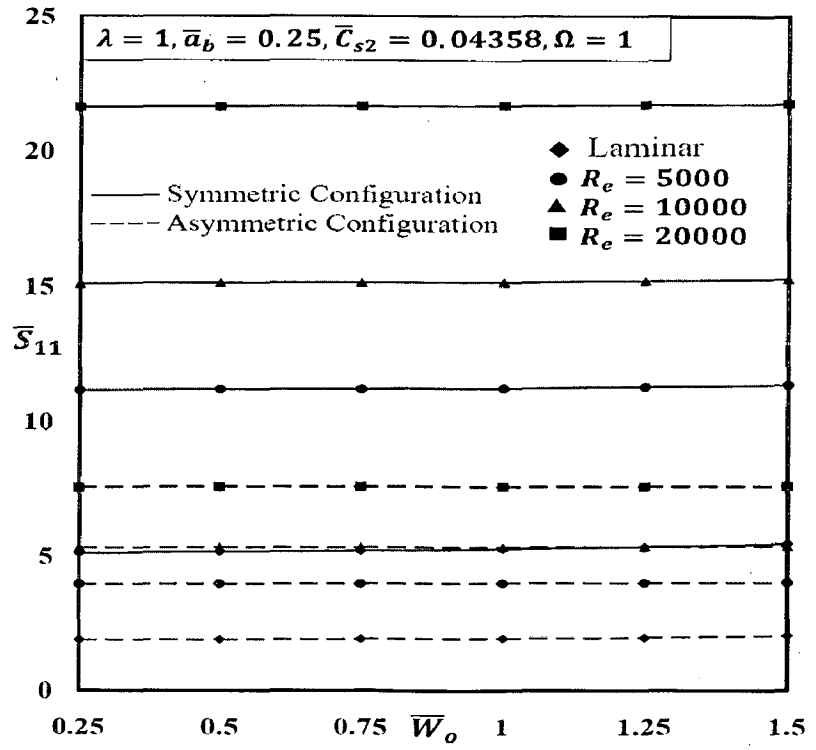

Fig. 4.5 Variation of with

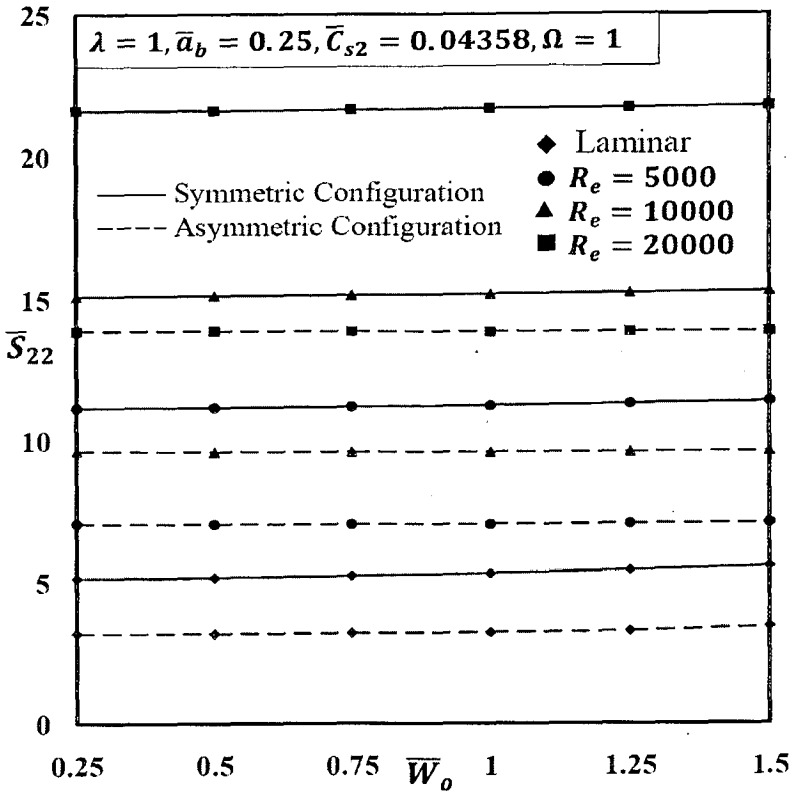

Fig. 4.6 Variation of with

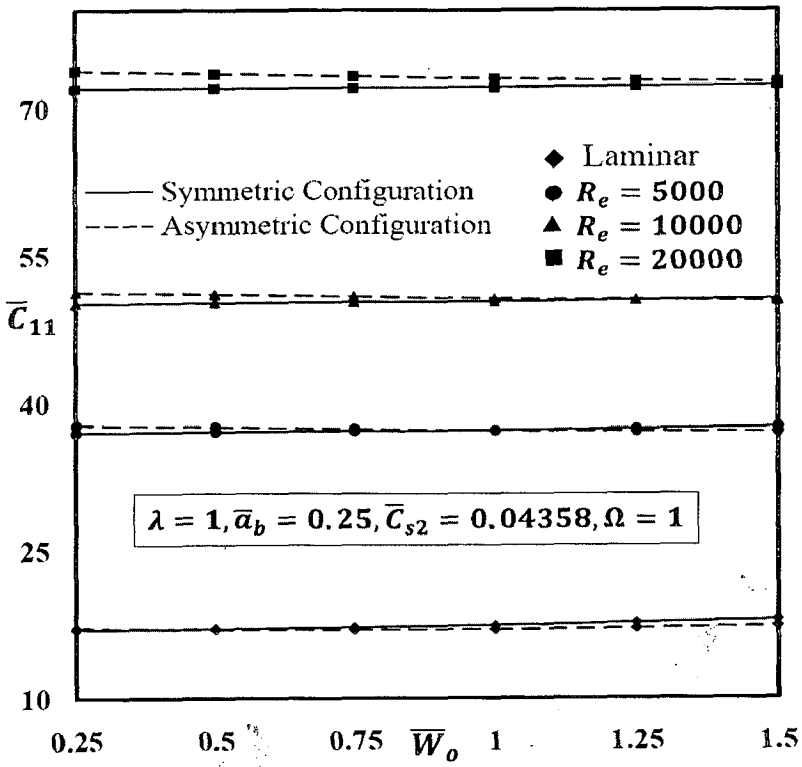

Fig. 4.7 Variation of with

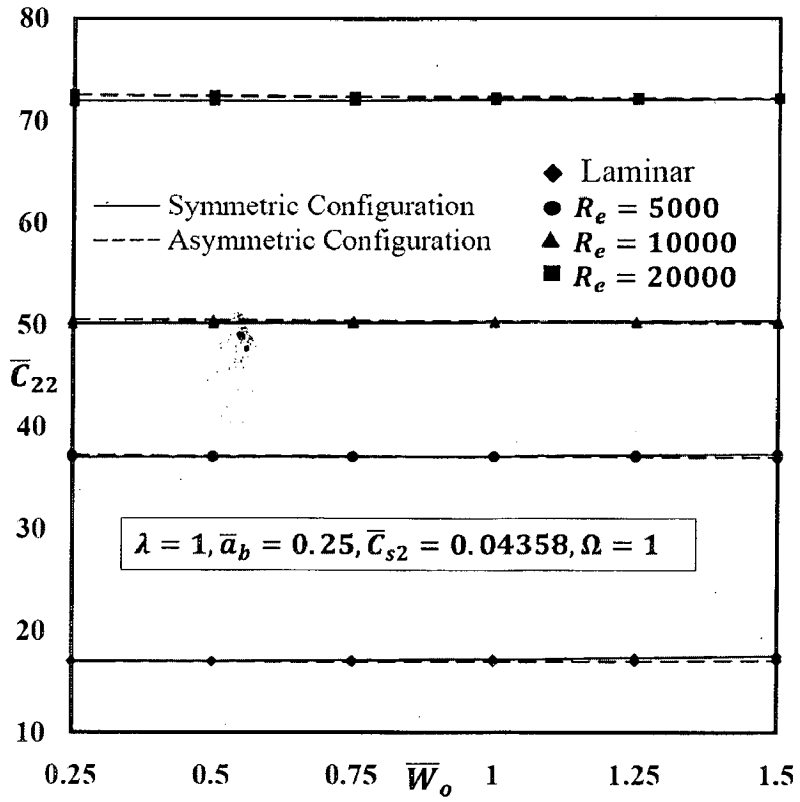

Fig. 4.8 Variation of with

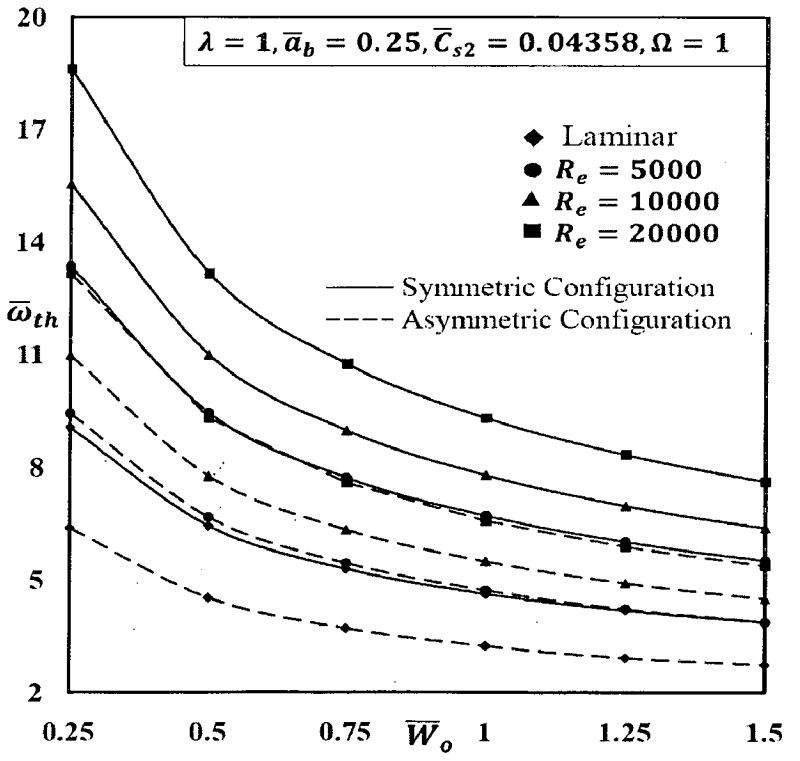

Fig. 4.9 Variation of with

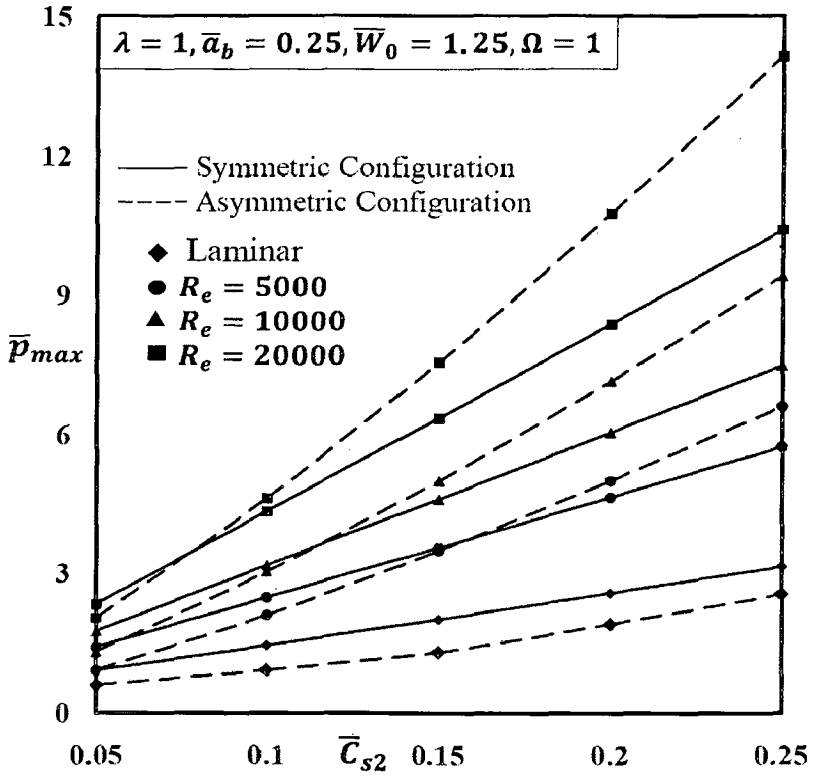

Fig. 4.10 Variation of with

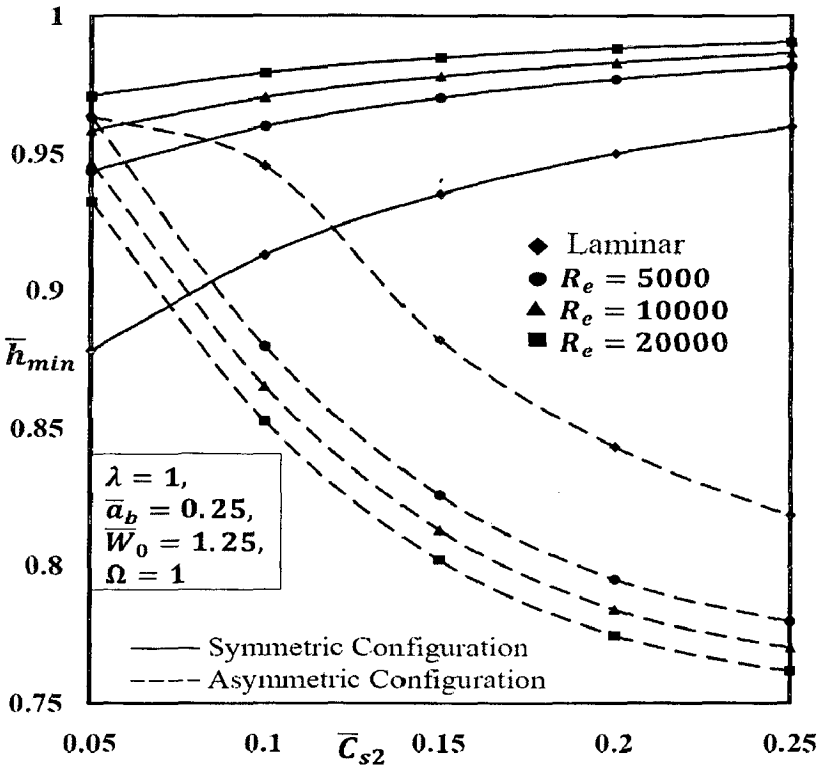

Fig. 4.11 Variation of with

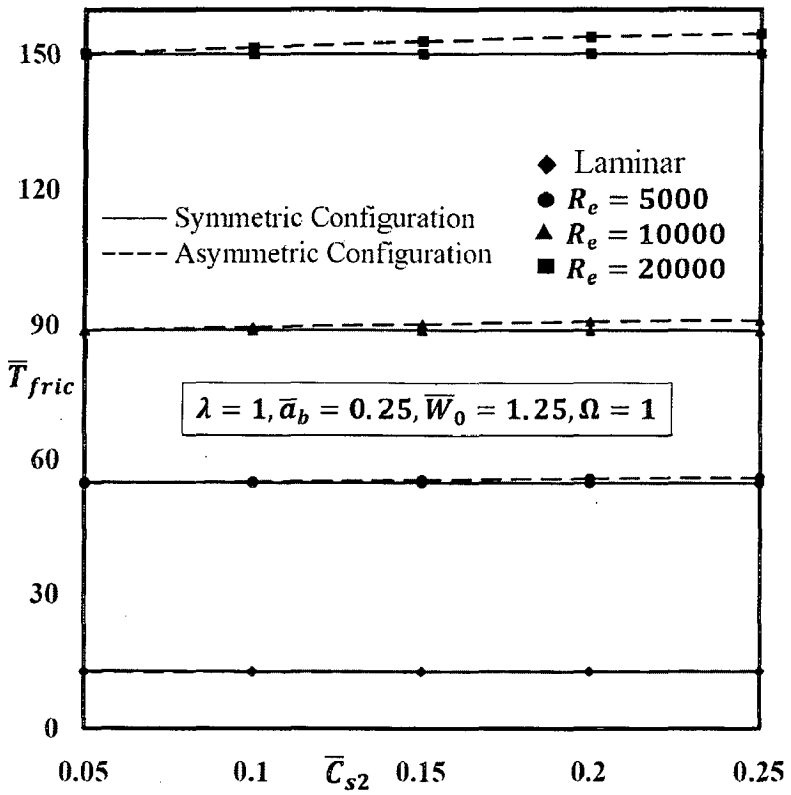

Fig. 4.12 Variation of with

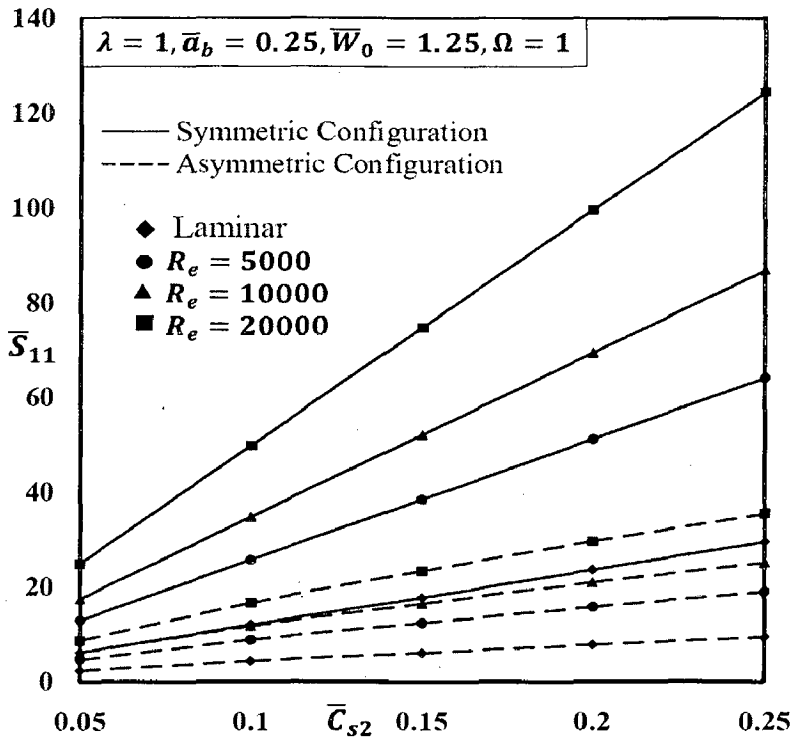

Fig. 4.13 Variation of with

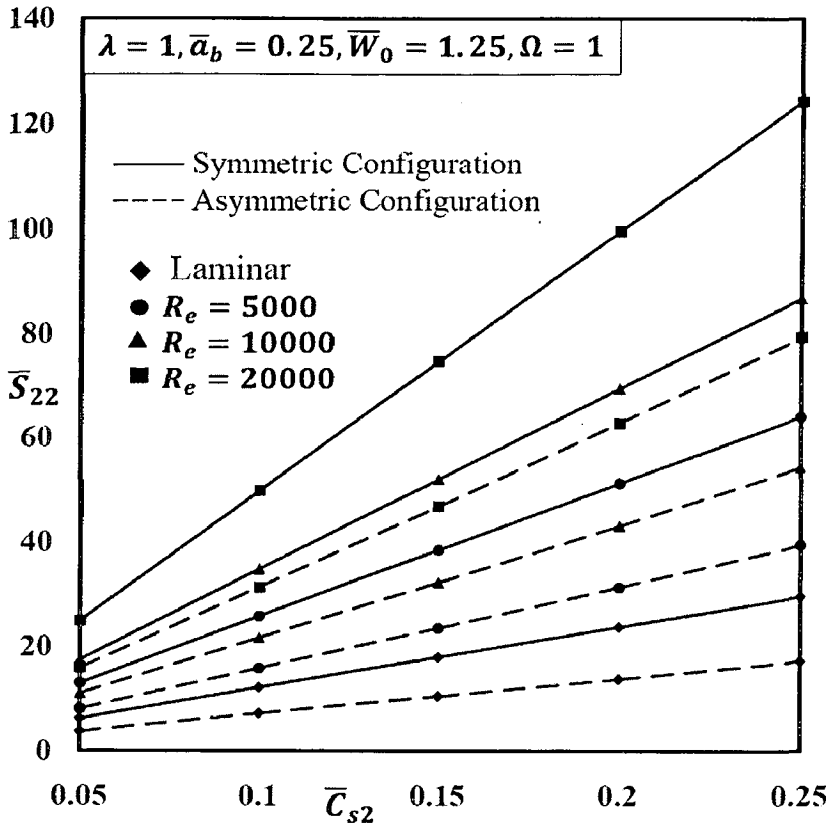

Fig. 4.14 Variation of with

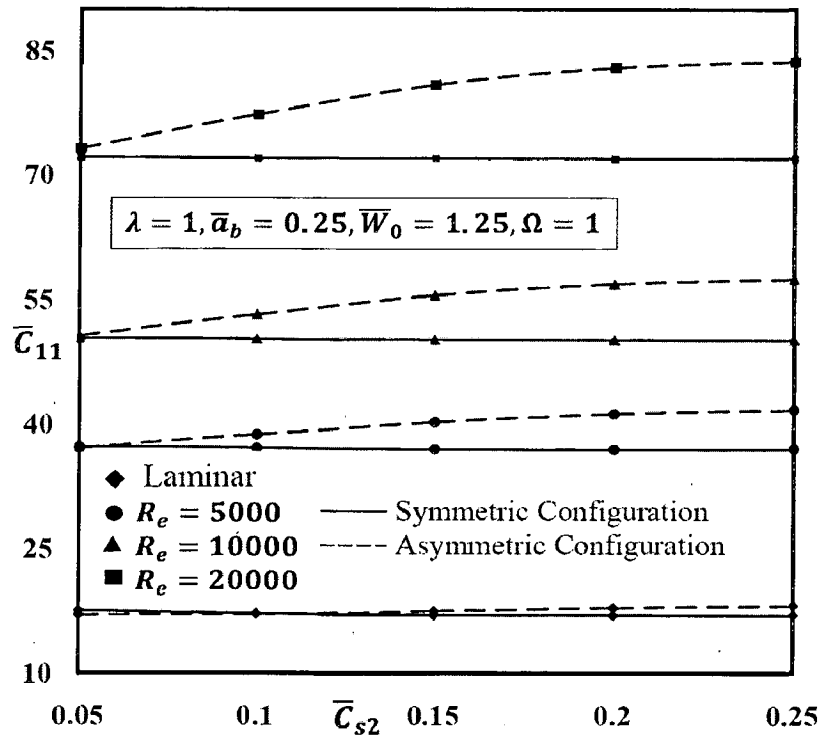

Fig. 4.15 Variation of with

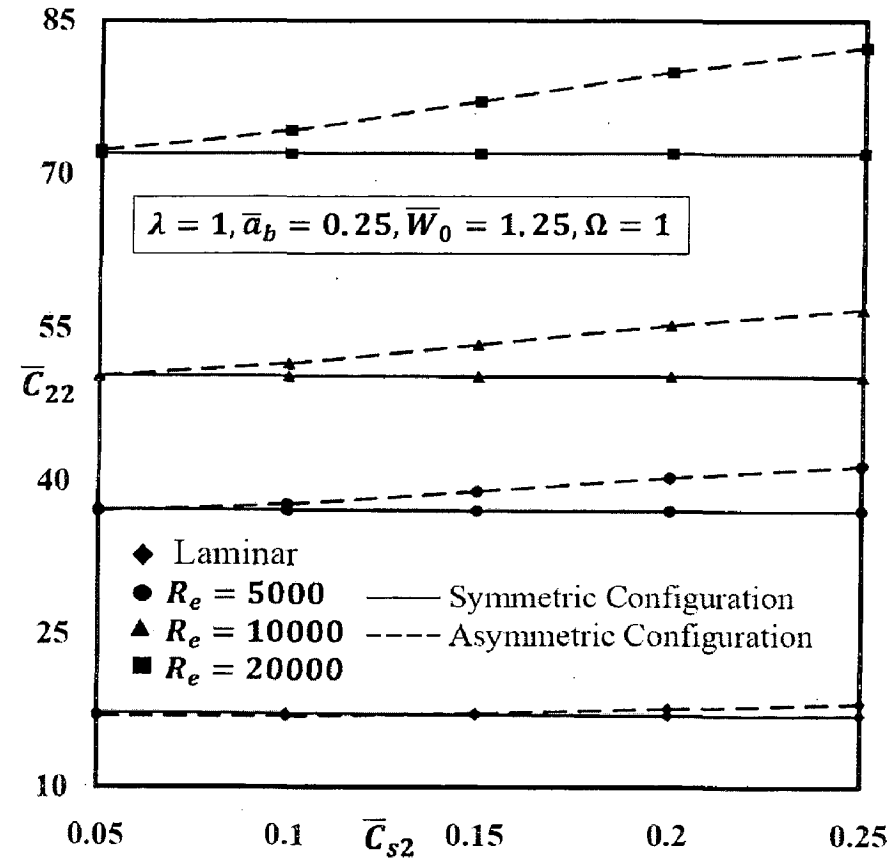

Fig. 4.16 Variation of with

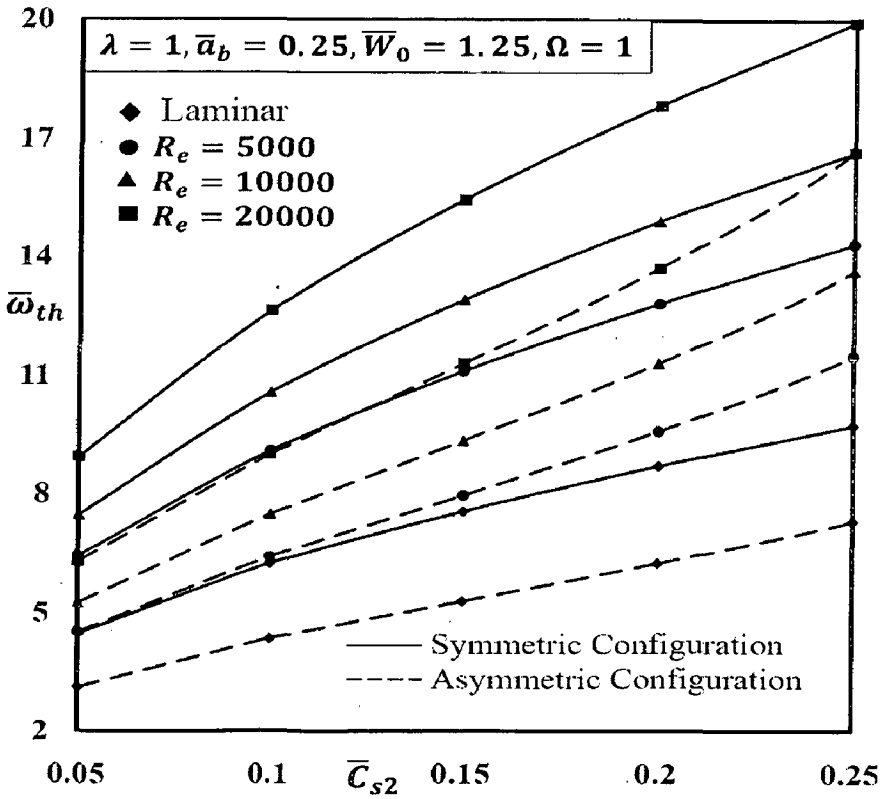

Fig. 4.17 Variation of with

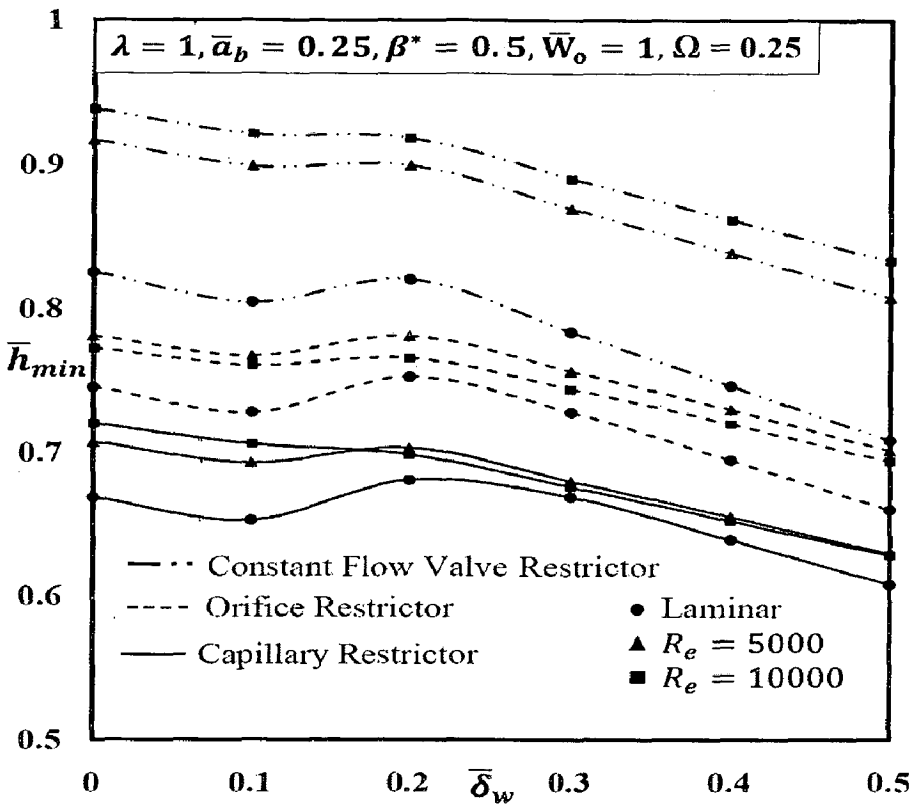

Fig. 4.18 Variation of with

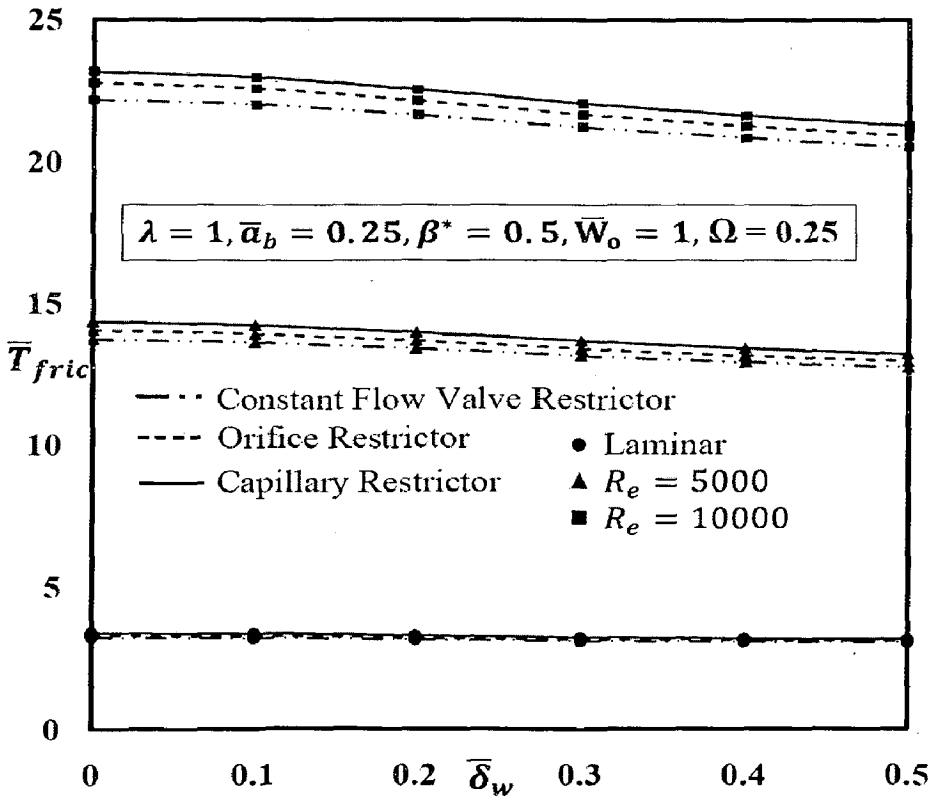

Fig. 4.19 Variation of with

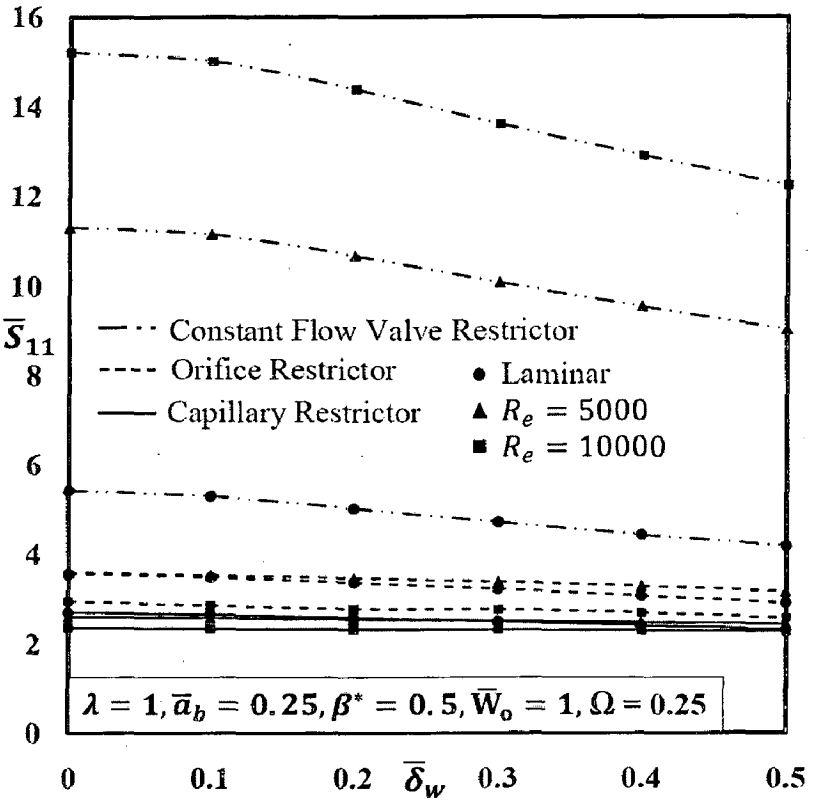

Fig. 4.20 Variation of with

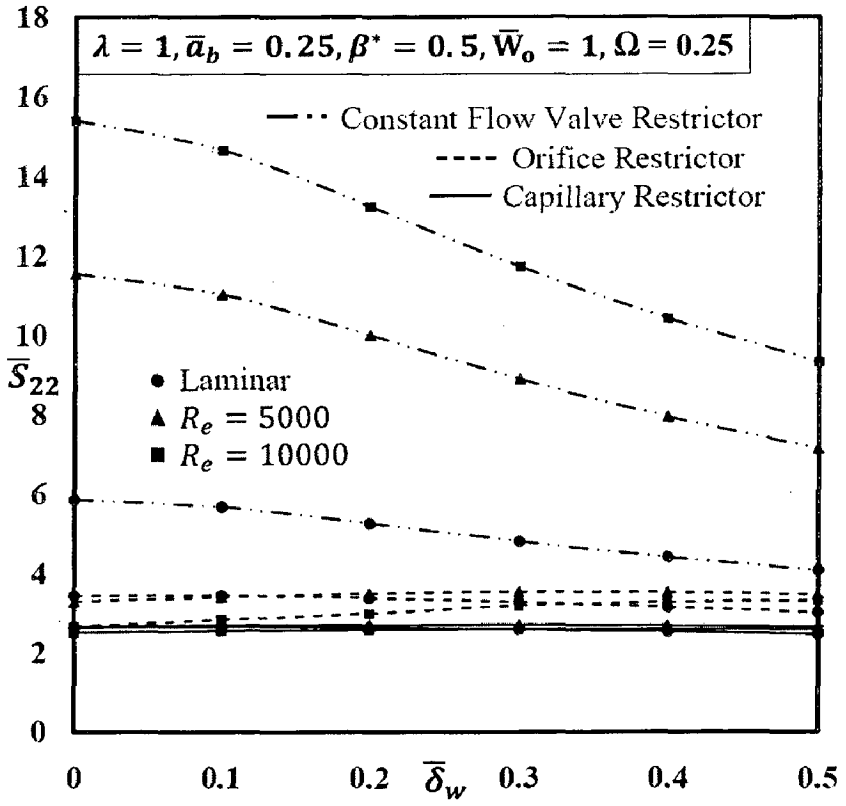

Fig. 4.21 Variation of with

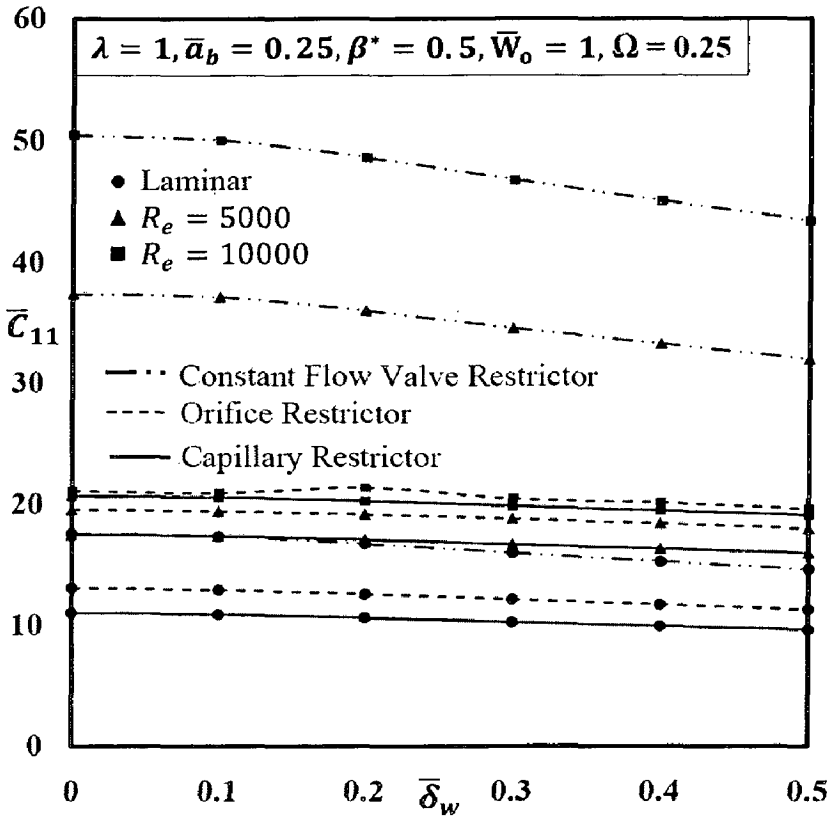

Fig. 4.22 Variation of with

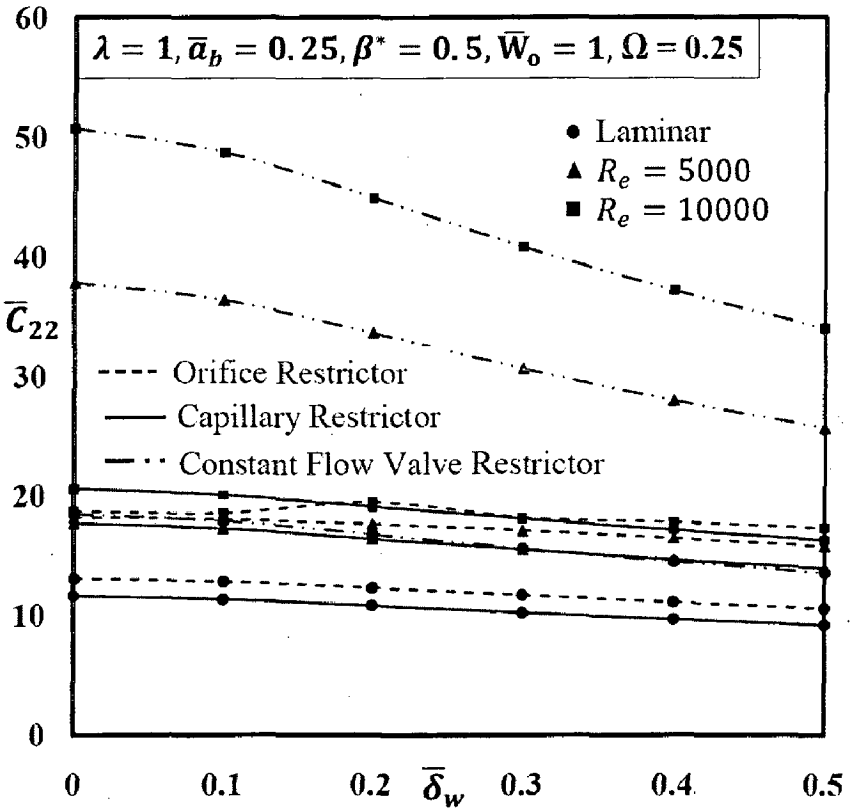

Fig. 4.23 Variation of with

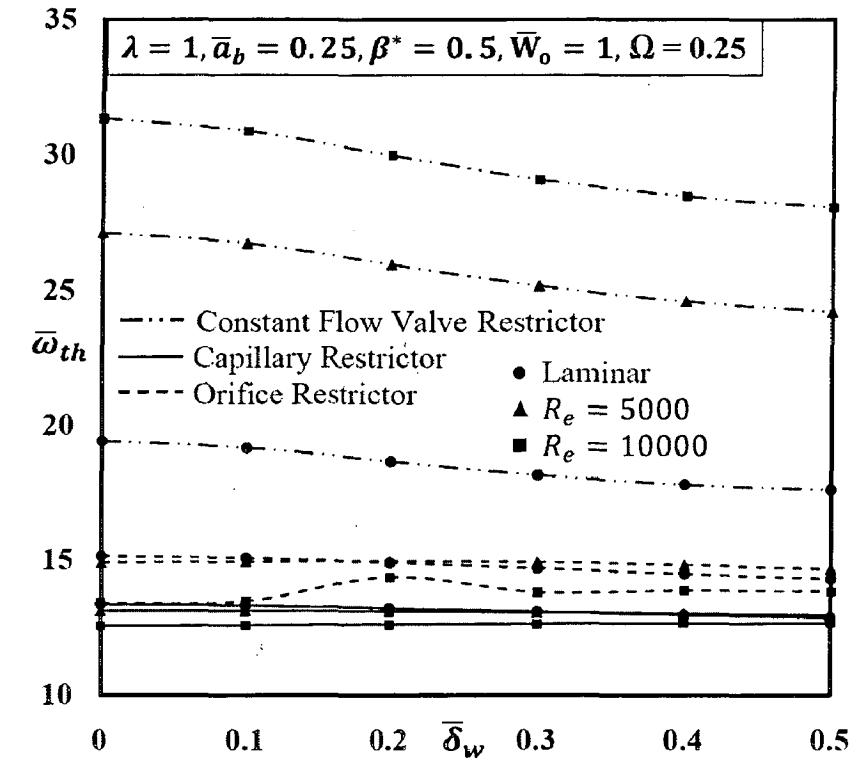

Fig. 4.24 Variation of with

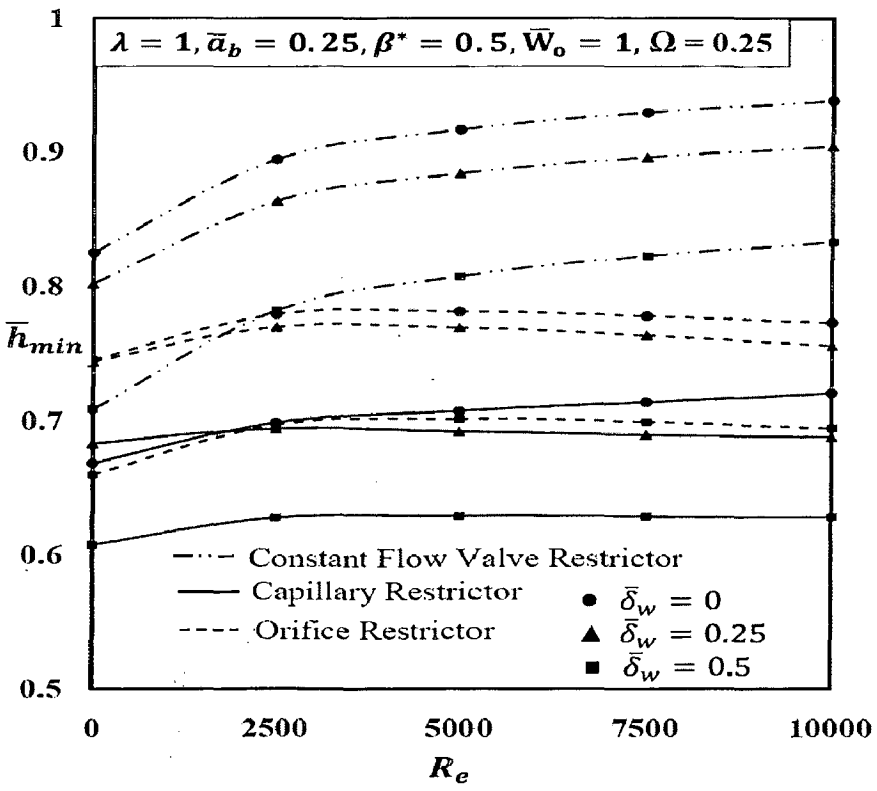

Fig. 4.25 Variation of with

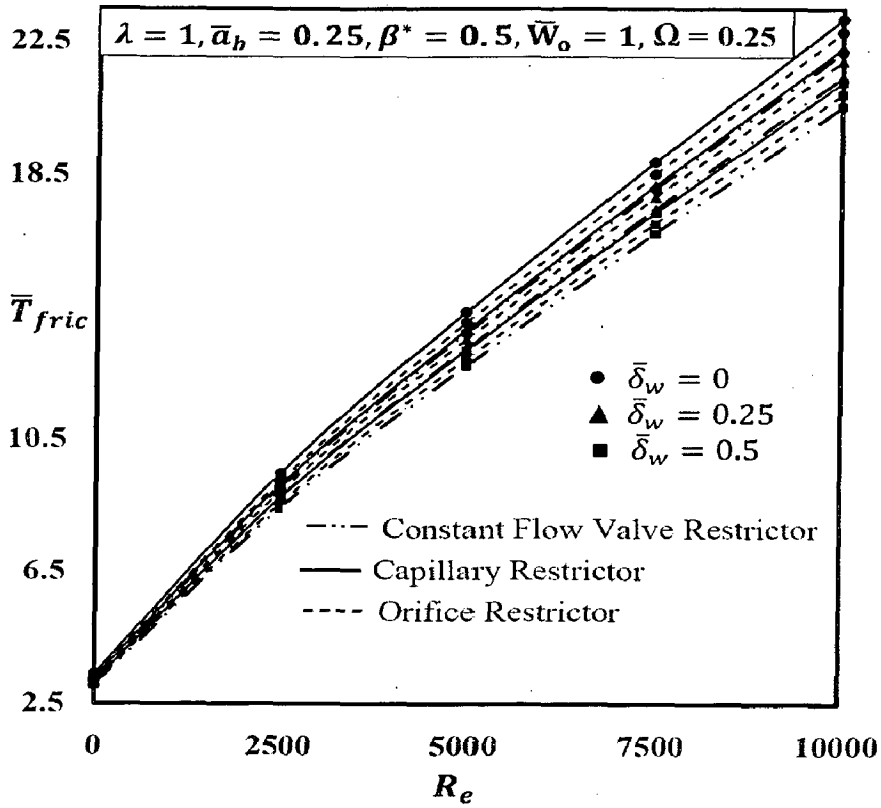

Fig. 4.26 Variation of with

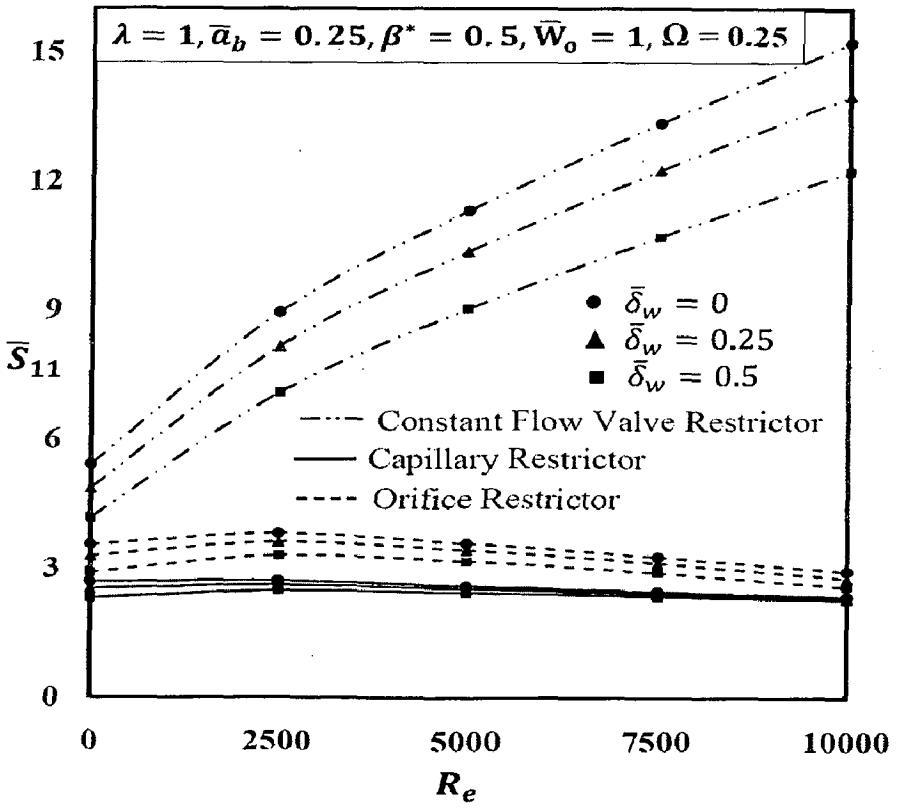

Fig. 4.27 Variation of with

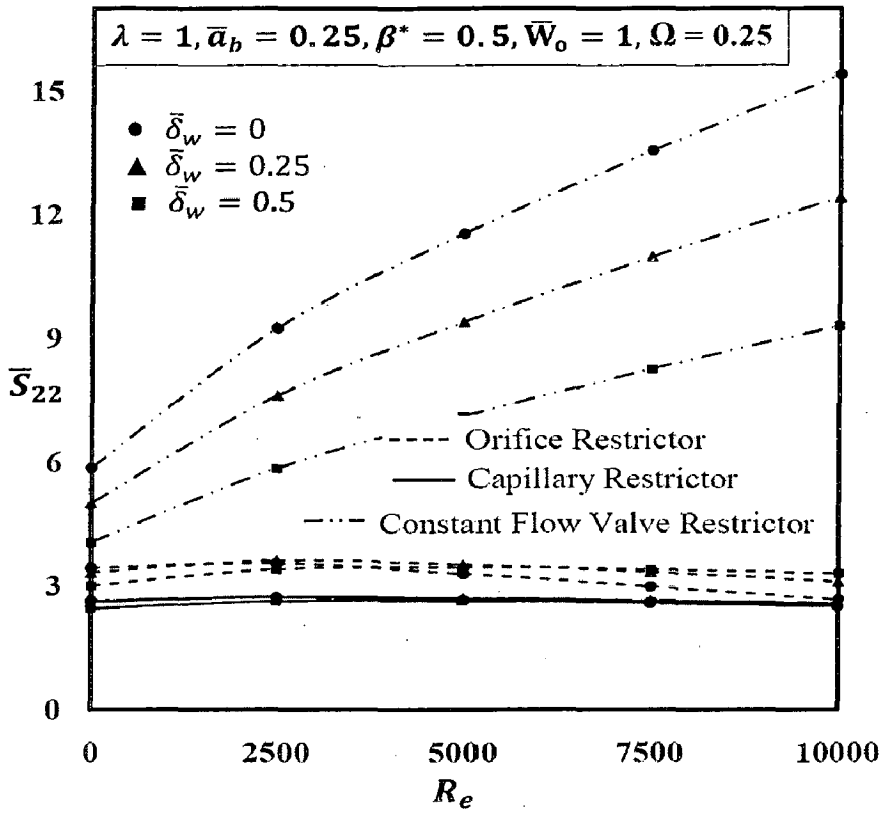

Fig. 4.28 Variation of with

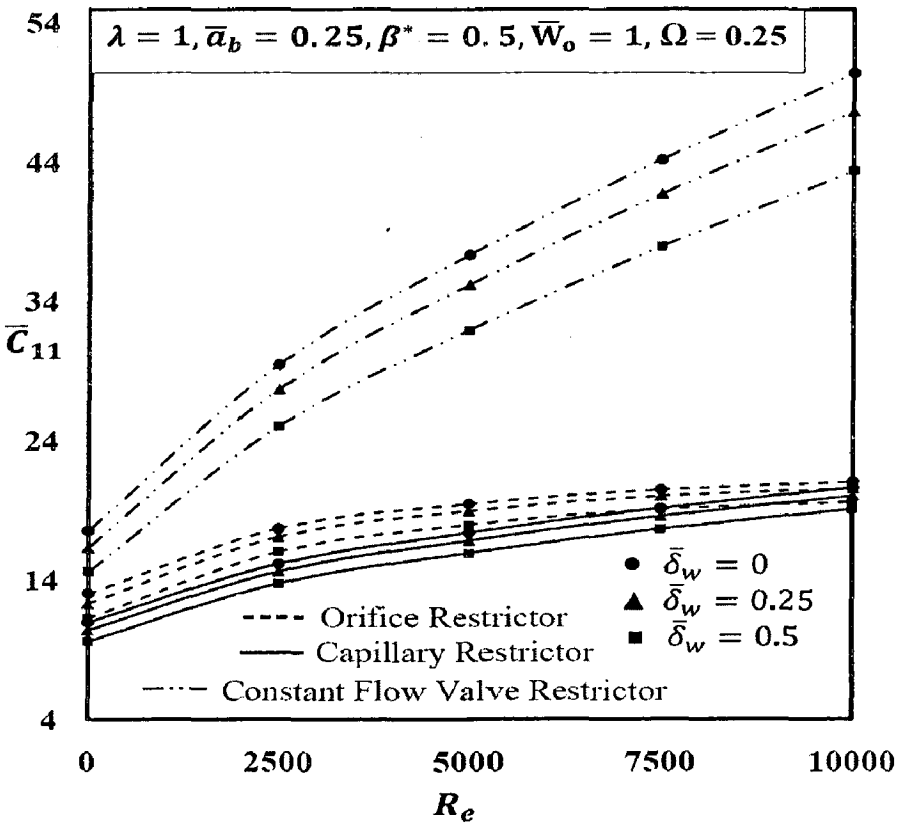

Fig. 4.29 Variation of with

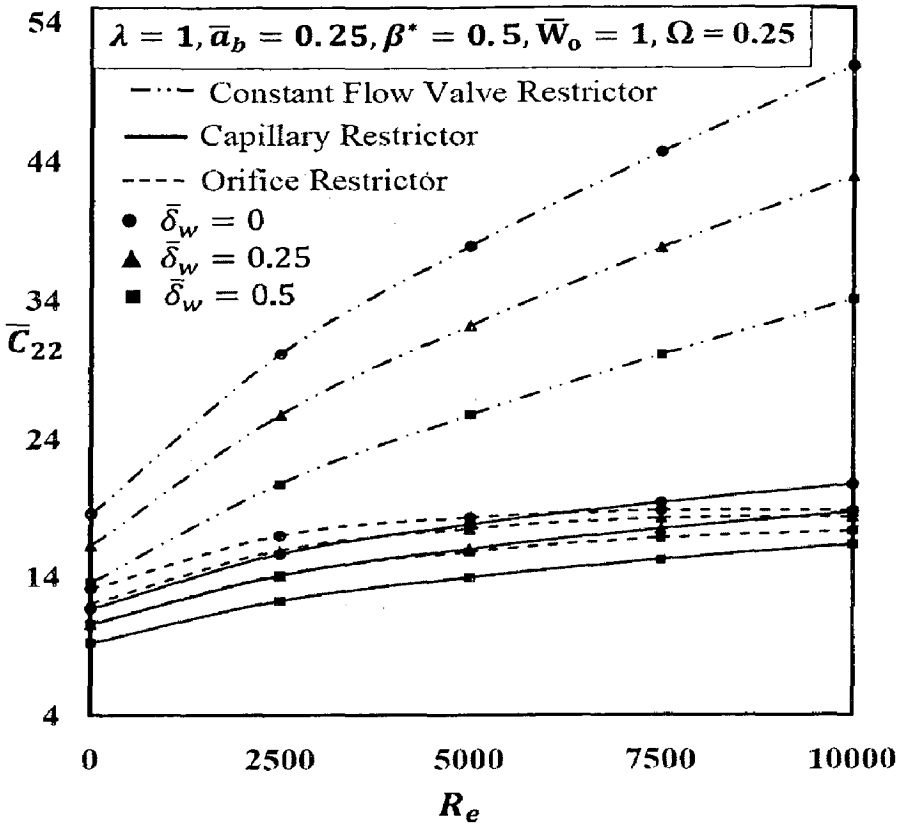

Fig. 4.30 Variation of with

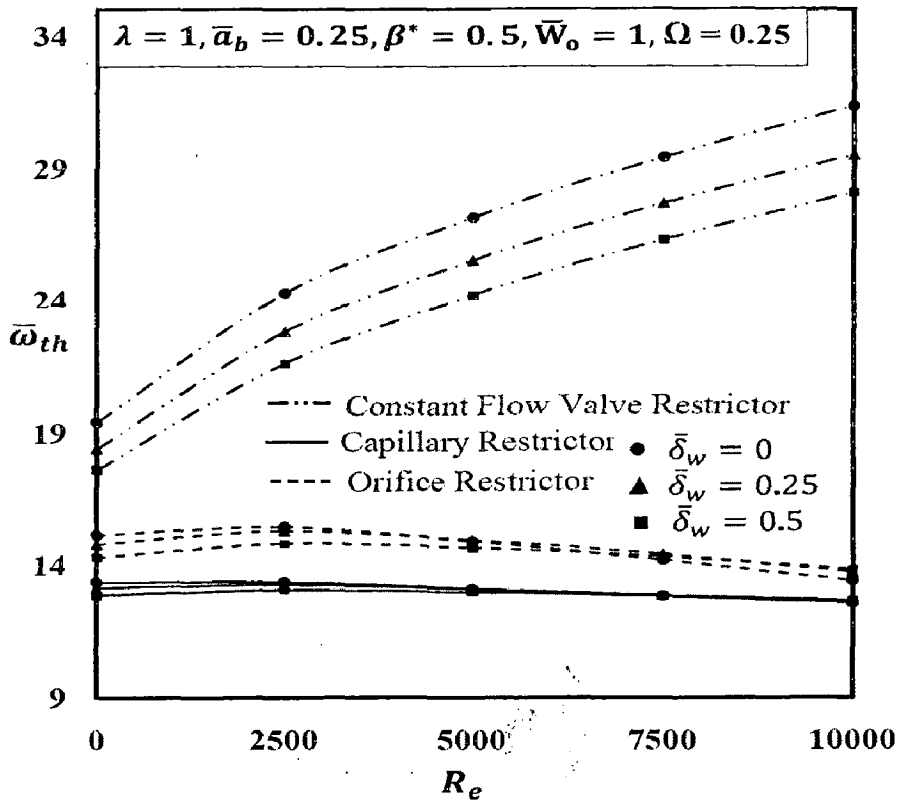

Fig. 4.31 Variation of with

Table 4.1

Bearing operating and geometric parameters

Parameters	Value
Bearing aspect ratio (λ)	1.0
Land width ratio ($\bar{a}_b$)	0.25
concentric design pressure ratio (β^*)	0.5
No. of rows of holes	2
No. of holes per row (Symmetric configuration)	12
No. of holes per row (Asymmetric configuration)	6
Reynolds number (R_e)	0 - 20000
External load ($\bar{W}_o$)	0.25 – 2.0
Restrictor design parameter ($\bar{C}_{s2}$)	0.05 – 0.25
Wear depth parameter ($\bar{\delta}_w$)	0 – 0.5

Table 4.2

Static and dynamic performance characteristics of worn/unworn non-recessed hole-entry hybrid journal bearing system operates in turbulent regime with different restrictors

	CONSTANT FLOW VALVE			
	$\bar{\delta}_w = 0, R_e = 0$		$\bar{\delta}_w = 0.5, R_e = 10000$	
	$\bar{C}_{s2} = 0.02$	$\bar{C}_{s2} = 0.1$	$\bar{C}_{s2} = 0.02$	$\bar{C}_{s2} = 0.1$
$\bar{p}_{max}$	0.5417	1.4025	0.9936	3.136
$\bar{h}_{min}$	0.7133	0.9165	0.7687	0.8772
$\bar{S}_{11}$	2.854	11.878	5.756	27.687
$\bar{S}_{22}$	3.292	12.13	4.574	20.733
$\bar{C}_{11}$	19.767	17.035	44.719	42.903
$\bar{C}_{22}$	20.466	17.318	34.673	33.442
$\bar{\omega}_{th}$	14.625	27.86	18.76	59.241
	ORIFICE RESTRICTOR			
	$\bar{\delta}_w = 0, R_e = 0$		$\bar{\delta}_w = 0.5, R_e = 10000$	
	$\bar{C}_{s2} = 0.02$	$\bar{C}_{s2} = 0.1$	$\bar{C}_{s2} = 0.02$	$\bar{C}_{s2} = 0.1$
$\bar{p}_{max}$	0.5281	0.9049	0.8778	1.3019
$\bar{h}_{min}$	0.6663	0.7475	0.7119	0.5991
$\bar{S}_{11}$	2.159	3.538	2.888	1.843
$\bar{S}_{22}$	2.45	3.129	2.943	2.531
$\bar{C}_{11}$	18.649	10.357	35.283	15.131
$\bar{C}_{22}$	18.44	9.975	28.296	12.648
$\bar{\omega}_{th}$	12.585	14.915	13.895	12.065
	CAPILLARY RESTRICTOR			
	$\bar{\delta}_w = 0, R_e = 0$		$\bar{\delta}_w = 0.5, R_e = 10000$	
	$\bar{C}_{s2} = 0.02$	$\bar{C}_{s2} = 0.1$	$\bar{C}_{s2} = 0.02$	$\bar{C}_{s2} = 0.1$
$\bar{p}_{max}$	0.5202	0.8063	0.8526	1.1978
$\bar{h}_{min}$	0.6239	0.6651	0.6823	0.6151
$\bar{S}_{11}$	1.775	2.686	2.413	2.154
$\bar{S}_{22}$	2.06	2.6	2.383	2.486
$\bar{C}_{11}$	18.143	10.417	32.866	18.085
$\bar{C}_{22}$	17.697	11.119	26.613	15.412
$\bar{\omega}_{th}$	11.503	13.309	12.611	12.38

λ=1.0, $\bar{a}_b$=0.25, β^*=0.5, $\bar{W}_o$=1.0, Ω =0.25

REFERENCES

[1]. **Yoshomoto S., Rowe W.B. and Ives D.,** "A Theoretical Investigation of the effect of inlet pocket size on the performance of hole-entry journal bearing employing capillary restrictors," Wear, Vol. 127, **1988,** pp.307-318.

[2]. **Rowe W.B. Xu S. Chon F.S. and Weston W.,** "Hybrid Journal Bearing with particular reference to hole-entry Configurations", Trib. Int., Vol.15, **1982,** pp.339-348.

[3]. **Stout K.J. and Rowe W.B.,** "Externally Pressurized bearing design for manufacture Part 3 design of liquid externally pressurized bearing for manufacture including tolerance Procedure", Trans. ASME, Jr. of Tribology , **1974,** pp 195-214.

[4]. **Rowe W.B. and Koshal D.,** "A new basis for the Optimization of hybrid journal bearing", Wear, Vol.64, **1980,** pp 115-131.

[5]. **Cheng K. and Rowe W.B.,** "A selection strategy for the design of externally pressurized journal bearings", Trib. Int. Vol. 28(7), **1995,** pp 465-474.

[6]. **Stout K.J. and Rowe W.B.,** "Externally pressurized bearings design for manufacture Part I journal bearing section", Trans. ASME, Jr. of Tribology, Vol. 7(3), **1974,** pp 98-106.

[7]. **Sharma. S.C., Sinhasan R. and Jain S.C.,** "An elastohydrostatic study of hole entry hybrid journal bearings with capillary restrictors", Trib. Intr. Vol. 26(2), **1993,** pp 93-107.

[8]. **Sharma S. C., Reddy N. Madhumohan,** "Influence of Elastic Effects on the Performance of Slot-Entry journal Bearings", Trib. Int. Vol.32, **1999,** pp 537-555.

[9]. **Sharma S.C., Kumar Vijay, Jain S.C., Subramanian M.,** "A Study of Slot-Entry Hydrostatic/hybrid Journal Bearing Using The finite Element Method", Trib. Int. Vol. 32, **1999,** pp 185-196.

[10]. **Jain S.C, Sharma Satish C. and Nagaraju T.,** "Misaligned Journal Effect in Liquid Hydrostatic Non- Recessed journal Bearings", WEAR, vol. 210, **1997,** pp. 67-75,.

[11]. **Sharma S.C., Kumar V., Jain S. C. and Nagaraju T.,** "Study of Hole-Entry Hybrid Journal Bearing System Considering Combined Influence of Thermal and Elastic Effects", Tribo. Int., vol. 36, **2003,** pp 903-920.

[12]. **Kumar V., Jain S.C and Sharma S.C.,** "Stability Margin of Hybrid Journal Bearing: influence of thermal and elastic effects", ASME J. Tribo., vol. 126, **2004,** pp. 630-634.

[13]. **Awasthi, R.K., Jain, S.C. and Sharma, S.C.,** "Finite Element Analysis of Orifice Compensated Multiple Hole-Entry Worn Hybrid Journal Bearing", Finite Elements in Analysis and Design, vol. 42(14-15), **2006**, pp. 1291-303.

[14]. **Awasthi, R.K., Sharma, Satish C. and Jain, S.C.** "Performance of Worn Non-Recessed Hole-Entry Hybrid Journal Bearings", Tribology International, vol. 40(5), **2007,** pp. 717-734.

[15]. **Ives D. and Rowe W.B.,** "The performance of hybrid journal bearing in the super laminar flow regimes:' DTLE Trib. Trans. Vol. 35(4), **1992,** pp 627-634.

[16]. **Constantinescu V. N.,**" Analysis of bearing operated in turbulent regime, "Jour. of Basic Engg., Trans of ASME, **1962,** pp.139-151.

[17]. **Constantinescu V. N.,**" On gas lubrication in turbulent regime," Jour. of Basic Engg. , Trans of ASME, **1964,** pp.475-482.

[18]. **Constantinescu V. N. and Galetuse S.,** "On the determination of friction forces in turbulent lubrication," ASLE Trans., Vol. 8, **1965**, pp.367-380.

[19]. **Constantinescu V. N.,** "Basic relationship in turbulent lubrication and their extension to thermal effects," Jour. of Lubr. Tech., Trans of ASME, **1973,** pp.147-154.

[20]. **Constantinescu V. N. and Galetuse S.,**" On the possibilities of improving the accuracy of the elevation of inertia forces in laminar and turbulent films," Jour. of Lubr. Tech., Trans of ASME, **1974,** pp.69-78.

[21]. **Galetuse S.,**" Experimental study on the interference of inertia and friction forces in turbulent lubrication," Jour. of Lubr. Tech., Trans of ASME, **1974,** pp.164-191.

[22]. **Constantinescu V. N. and Galetuse S.,**" Operating characteristics of journal bearings operating in turbulent inertial flow," Jour. of Lubr. Tech., Trans of ASME, **1982,** pp.173-179.

[23]. **Ng C. W. and Pan C.H.T.,**" A linearized turbulent lubrication theory," Jour. of Basic Engg., **1965**, pp.675-.688.

[24]. **Elrod H. G.**, "A general theory for laminar lubrication with Reynolds roughness," Jour. of Lubr. Tech., Trans of ASME, Vol.101, **1979,** pp.8-14.

[25]. **Hirs G. G.,**" A bulk flow theory for turbulence in lubricant films," Jour. of Lubr. Tech., Trans of ASME, **1973,** pp.137-146.

[26]. **Hirs G. G.,**"A systematic study of turbulent film flow" Trans of ASME, **1974,** pp.118-126.

[27]. **Burton R.A.**, "Approximation in turbulent film analysis," Jour. of Lubr. Tech., Trans of ASME, **1974,** pp.103-109.

[28]. **Burton R. A. and Hsu Y. C.**, "The incompressible turbulent thin film short bearing with inertial effects," Trans of ASME, **1974,** pp.158-163.

[29]. **Taylor C.M. and Dowson D.,** "Turbulent lubrication theory application to design," Trans of ASME, **1974,** pp.36-47.

[30]. **Vinay Kumar**, " Theoretical hydrodynamic load capacity of an axially undefined full porous journal bearing in the turbulent regime considering slip flow and curvature, "Elsevier Sequoia S.A., Wear, Vol. 65, **1981**, pp. 277-284.

[31]. **Vinay Kumar**, "Plain hydrodynamic bearing in the turbulent regime- A critical review," Elsevier Sequoia S.A., Wear, Vol. 72, **1981**, pp. 13-28.

[32]. **Vinay Kumar**," Hydrodynamic instability of self acting journal bearings of finite length in the turbulent regime," Elsevier Sequoia S.A., Wear, Vol. 88, **1983**, pp. 133-143.

[33]. **Vohr J. H. and Mein-kai Ho,** "Application of energy model of turbulence to calculation of lubricant flows," Jour. of Lubr. Tech., Trans. of ASME, **1974,** pp.95-105.

[34]. **Vohr J. H., Smalley A. J., Castelli V. and Wachmann C.**," An analytical and experimental investigation of turbulent flow in bearing films including the effects of convective fluid inertia forces, "Jour. of Lubr. Tech., Trans. of ASME, **1974,** pp.151-157.

[35]. **Hashimoto H. and Wada S.,**" Turbulent lubrication of tilting-pad thrust bearings with thermal and elastic deformations, "Jourl. of Trib., Trans. of ASME, Vol. 107, **1985**, pp.82-86.

[36]. **Hashimoto H., Wada S. and Jin-ichi Ito,**" An application of short bearing theory to dynamic characteristic problems of turbulent journal bearings," Jourl. of Trib., Trans. of ASME, Vol. 109, **1985**, pp.307-314.

[37]. **Hashimoto H. and Wada S.,**" Theoretical approach to turbulent lubrication problems including surface roughness effects, "Jourl. of Trib., Trans. of ASME, Vol. 107, **1989**, pp.17-22.

[38]. **Hashimoto H.,**" The effects of "O-Type" cavitation on the static and dynamic characteristics of turbulent journal bearings, "Trib. Trans., Vol.34, **1991**, pp.100-106.

[39]. **Kumar A. and Mishra S. S.,**" steady state analysis of non-circular worn journal bearings in nonlaminar lubrication regimes, "Trib. Int., Vol. 29, **1996**, pp. 493-498.

[40]. **Luis san Andres**, "Turbulent hybrid bearings with fluid inertia effects, "Jourl. of Trib., Trans. of ASME, Vol. 112, **1990**, pp.699-707.

[41]. **Yu T. S. and Szeri A. Z.,**" Partial journal bearing performance in the laminar regime," Jour. of Lubr. Tech., Trans. of ASME, **1975,** pp.94-100.

[42]. **Wilcock D. F. and Pinkus O.,**" Effect of turbulence and viscosity variation on the dynamic coefficients of fluid film journal bearings," Jourl. of Trib., Trans. of ASME, Vol. 102, **1985**, pp.256-261.

[43]. **Tieu A. K. and Kosasih P. B.,**" A transition turbulent lubrication theory using mixing length concept," Jourl. of Trib., Trans. of ASME, Vol. 115, **1993**, pp.591-596.

[44]. **Chun S. M. and Ha S. H.,**" Study on mixing flow effects in a high-speed journal bearing," Tribology International, Vol. 34 , **2001**, pp. 397–405.

[45]. **Frene J., Arghir M. and Constantinescu V.,**" Combined thin-film and Navier–Stokes analysis in high Reynolds number lubrication," Tribology International, Vol. 39, **2006**, pp.734–747.

[46]. **Jian C. W. C. and Chen C. K.,**" Bifurcation and chaos analysis of a flexible rotor supported by turbulent long journal bearings," Elsevier Science, Chaos Solitons and Fractals, Vol. 34, **2007**, pp. 1160–1179.

[47]. **Shenoy S. B. and Pai R.,** "Theoretical investigations on the performance of an externally adjustable fluid-film bearing including misalignment and turbulence effects," Tribology International, Vol. 42, **2009**, pp. 1088–1100.

[48]. **E. Rajasekhar Nicodemus and Satish C. Sharma,** "A study of worn hybrid journal bearing system with different recess shapes under turbulent regime," ASME Jr. of Tribo., Vol. 132, **2010**, pp.1-12.

[49]. **Dufrane K. F., Kannel J. W. and. McCloskey T. H,** "Wear of steam turbine journal bearings at low operating speeds," ASME Jr. Lubr. Tech., Vol. 105, **1983**, pp. 313–317.

[50]. **Duckworth W. E. and Forrester P. B.,** "Wear of lubricated journal bearings," proc. inst. mech. eng. London, conference on lubrication and wear, **1957**, pp. 714-719.

[51]. **Forrester P. B.,** "Bearings and journal wear," Symposium on Wear in Gasoline Engine, Thornton Research Centre, **1960**, pp. 75-91.

[52]. **Hashimoto H., Wada S. and Nojima K.,** "Performance characteristics of worn journal bearings in both laminar and turbulent regimes. Part I: Steady-State characteristics". ASLE Trans., Vol. 29(4), **1986**, pp.565-571.

[53]. **Vaidyanathan K. and Keith T. G.,** "Numerical prediction of cavitation in non circular journal bearings," Trob. Trans., Vol 32, **1989**, pp.215-224.

[54]. **Jain S. C., Sinhasan R. and Sharma S. C.,** "Analytical study of a flexible hybrid journal bearing system using different flow control devices". Tribo. Intn., Vol. 25, **1992**, pp.387-395.

[55]. **Kumar A. and Rao N. S.,** "Steady state performance of finite hydrodynamic porous journal bearings in turbulent regimes". Wear, Vol. 167, **1993**, pp. 121-126.

[56]. **Kumar A. and Mishra S. S.,** "Steady state analysis of non-circular worn journal bearings in nonlaminar lubrication regimes". Tribo. Intn., Vol. 29, **1996**, pp. 493-498.

[57]. **Fillon M. and Bouyer J.,** "Thermo hydrodynamic analysis of a worn plain journal bearing," Trib. Int., Vol. 37, **2004**, pp. 129-136.

[58]. **Chris A. Papadopoulos, Pantelis G. Nikolakopoulos and George D. Gounaris,** "Identification of clearances and stability analysis for a rotor-journal bearing system," Mechanism and Machine Theory, Vol. 43, **2008**, pp. 411–426.

[59]. **Gertzos K.P., Nikolakopoulos P.G., Chasalevris A.C. and Papadopoulos C.A.,** "Wear identification in rotor-bearing systems by measurements of dynamic bearing characteristics," computers and structures, Vol. 89, **2011**, pp. 55-56.

[60]. **Soni S. C., Sinhasan R. and Singh D. V.,** "Analysis by the finite element method of hydrodynamic bearings operating in the laminar and superlaminar regimes," Elsevier Sequoia, wear, Vol. 84, **1983**, pp.285 – 296.

[61]. **Cameron A.,** "The principle of lubrication," Longmans Green and co. Ltd. London, **1968.**

[62]. **Rowe W. B.,** "Hydrostatic and hybrid bearing design," Butter worth, London, **1983.**

PUBLICATIONS FROM THE PRESENT WORK

[1]. **Ram N., Sankla D. and Sharma S. C.,** "A study of a constant flow valve compensated non-recessed hole-entry hybrid journal bearing operating in turbulent regime," Published in proceedings of 66th STLE annual meeting held at Atlanta, U. S., May 15-19, **2011.**

[2]. **Ram N., Sankla D. and Sharma S. C.,** "Performance of An Orifice Compensated Non-Recessed Hole-Entry Hybrid Journal Bearing Operating In Turbulent Regime," Proceedings of the ASME International Design Engineering Technical Conferences & Computers and Information in Engineering Conference (IDETC/CIE), Washington, DC, USA, August 28-31, **2011.**